

Neutral and Anionic Silyl Hydride Derivatives of the Tantalum Imido Fragment $\text{Cp}^*(\text{DippN}=\text{)Ta}$ ($\text{Cp}^* = \eta^5\text{-C}_5\text{Me}_5$; $\text{Dipp} = 2,6\text{-}^i\text{Pr}_2\text{C}_6\text{H}_3$). Reactive σ -Bonds and Intramolecular C–H Bond Activations Involving the Silyl Ligands

Urs Burckhardt, Gary L. Casty, John Gavenonis, and T. Don Tilley*

Department of Chemistry, University of California, Berkeley, Berkeley, California 94720-1460

Received April 22, 2002

The syntheses and reactivities of alkyl, silyl, and hydride complexes of the type $\text{Cp}^*(\text{DippN}=\text{)TaRR}'$ ($\text{Cp}^* = \eta^5\text{-C}_5\text{Me}_5$; $\text{Dipp} = 2,6\text{-}^i\text{Pr}_2\text{C}_6\text{H}_3$; $\text{R} = \text{silyl, alkyl}$; $\text{R}' = \text{alkyl, hydride}$) are described. The compounds $\text{Cp}^*(\text{DippN}=\text{)Ta}(\text{SiR}_3)\text{Cl}$ ($\text{SiR}_3 = \text{Si}(\text{SiMe}_3)_3$ (**1**), SiPh_3 (**2**), SiHMe_2 (**3**); $\text{Mes} = 2,4,6\text{-Me}_3\text{C}_6\text{H}_2$), prepared from $\text{Cp}^*(\text{DippN}=\text{)TaCl}_2$ and $(\text{THF})_n\text{LiSiR}_3$, react with H_2 to yield the dimeric hydride $[\text{Cp}^*(\text{DippN}=\text{)TaCl}(\mu\text{-H})_2]$ (**4**). The reaction of **4** with $(\text{THF})_3\text{LiSi}(\text{SiMe}_3)_3$ (2 equiv) gave the 16-electron silyl hydride complex $\text{Cp}^*(\text{DippN}=\text{)Ta}[\text{Si}(\text{SiMe}_3)_3]\text{H}$ (**6**), which is Lewis acidic and reversibly binds halide ions to afford anionic Ta(V) complexes of the type $\text{A}^+\{\text{Cp}^*(\text{DippN}=\text{)Ta}(\text{X})[\text{Si}(\text{SiMe}_3)_3]\text{H}\}^-$ ($\text{A} = \text{Li}(\text{THF})_3$, $\text{X} = \text{Cl}$ (**5**); $\text{A} = \text{NBu}_4$, $\text{X} = \text{Br}$ (**7**) and I (**8**)). For complexes **5**, **7**, and **8**, NMR and X-ray data suggest the presence of weak three-center interactions involving Ta, Si, and H. Silyl hydride **6** reacts with xylyl isocyanide (xylyl = 2,6-dimethylphenyl) and acetonitrile to give the corresponding η^2 -silimine and azomethine insertion products, respectively, while treatment with acetone yields the stable isopropoxide product arising from insertion into the Ta–H bond. When complex **6** is treated with ethylene or diphenylacetylene, elimination of $\text{HSi}(\text{SiMe}_3)_3$ occurs, along with formation of a five-membered tantalacycle resulting from coupling of the unsaturated substrate at Ta. Hydrogenolysis of **6** yields $\text{HSi}(\text{SiMe}_3)_3$ and a dimeric dihydride $[\text{Cp}^*(\text{DippN}=\text{)TaH}(\mu\text{-H})_2]$ (**14**). At room temperature, **6** rearranges ($t_{1/2} = 8.5$ h) to an unusual alkyl hydride species resulting from C–H bond activation, $\text{Cp}^*(\text{DippN}=\text{)Ta}[\text{CH}_2\text{Si}(\text{SiMe}_3)_2\text{SiMe}_2\text{H}]\text{H}$ (**15**). This complex exhibits a γ -agostic Si–H interaction with the metal center. An attempt to prepare $\text{Cp}^*(\text{DippN}=\text{)Ta}(\text{SiHMe}_2)\text{H}$ produced the alkyl hydride product $\text{Cp}^*(\text{DippN}=\text{)Ta}[\eta^2\text{-CH}_2(2\text{-SiH}_2\text{Mes-3,5-Me}_2\text{C}_6\text{H}_2)]\text{H}$ (**20**), which apparently results from decomposition of the expected silyl hydride. The alkyl hydride complex $[\text{Cp}^*(\text{DippN}=\text{)TaMe}(\mu\text{-H})_2]$ (**25**) was prepared by the hydrogenolysis of $\text{Cp}^*(\text{DippN}=\text{)Ta}[\text{Si}(\text{SiMe}_3)_3]\text{Me}$ (**23**), whereas $\text{Cp}^*(\text{DippN}=\text{)Ta}(\text{CH}_2\text{CMe}_3)\text{H}$ (**26**) was obtained by treatment of **4** with NpMgCl . Complex **26** possesses an α -agostic C–H interaction, and the corresponding deuteride **26-d** slowly scrambles deuterium into the methylene positions.

Introduction

Early transition metal silicon chemistry is receiving increasing attention, especially with the discovery of processes for the catalytic hydrosilylation of olefins^{1–5} and the polymerization of hydrosilanes.^{6–8} Work in our laboratory has centered on group 4 d^0 metallocene

derivatives,^{6,9–11} since such complexes have proven to be precursors to the best dehydropolymerization catalysts. Given the proven potential for chemical transformations mediated by early transition metals, considerable interest has focused on the development of catalysts featuring ancillary ligands other than cyclopentadienyl groups.^{6,9,10} In this context the formal 1σ , 2π donor analogy between cyclopentadienyl $[\eta^5\text{-C}_5\text{R}_5]^-$ and imido $[\text{RN}=\text{}]^-$ ligands^{12–16} suggests that complexes based on

(1) Fu, P.-F.; Brard, L.; Li, Y.; Marks, T. J. *J. Am. Chem. Soc.* **1995**, *117*, 7157.

(2) Gountchev, T. I.; Tilley, T. D. *Organometallics* **1999**, *18*, 5661.

(3) Carter, M. B.; Schiott, B.; Butierrez, A.; Buchwald, S. L. *J. Am. Chem. Soc.* **1994**, *116*, 11667.

(4) Molander, G. A.; Julius, M. *J. Org. Chem.* **1992**, *57*, 6347.

(5) Molander, G. A.; Dowdy, D. E.; Noll, B. C. *Organometallics* **1998**, *17*, 3754.

(6) Tilley, T. D. *Acc. Chem. Res.* **1993**, *26*, 22.

(7) Gauvin, F.; Harrod, J. F.; Woo, H. G. *Adv. Organomet. Chem.* **1998**, *42*, 363.

(8) Corey, J. In *Advances in Silicon Chemistry*; Larson, G., Ed.; JAI Press: Greenwich, CT, 1991; Vol. 1, p 327.

(9) Woo, H.-G.; Walzer, J. F.; Tilley, T. D. *J. Am. Chem. Soc.* **1992**, *114*, 7047.

(10) Imori, T.; Tilley, T. D. *Polyhedron* **1994**, *13*, 2231.

(11) Woo, H.-G.; Tilley, T. D. *J. Am. Chem. Soc.* **1989**, *111*, 3757.

(12) Williams, D. S.; Schofield, M. H.; Anhaus, J. T.; Schrock, R. R. *J. Am. Chem. Soc.* **1990**, *112*, 6728.

(13) Williams, D. S.; Anhaus, J. T.; Schofield, M. H.; Schrock, R. R.; Davis, W. M. *J. Am. Chem. Soc.* **1991**, *113*, 5480.

(14) Williams, D. S.; Schrock, R. R. *Organometallics* **1993**, *12*, 1148.

imido ligands might represent interesting candidates for investigation. We have therefore targeted the synthesis and study of d^0 imido complexes containing reactive M–R (R = H, silyl) σ -bonds.^{17–20} These investigations have produced d^0 bis(imido) silyl complexes of molybdenum and tungsten, and attempts to generate hydride derivatives in this system revealed that the silyl hydrides (DippN=)₂M[Si(SiMe₃)₃]H (Dipp = 2,6-*i*-Pr₂C₆H₃, M = Mo, W) are highly unstable and degrade via an interesting β -silyl elimination of HSiMe₃.¹⁸

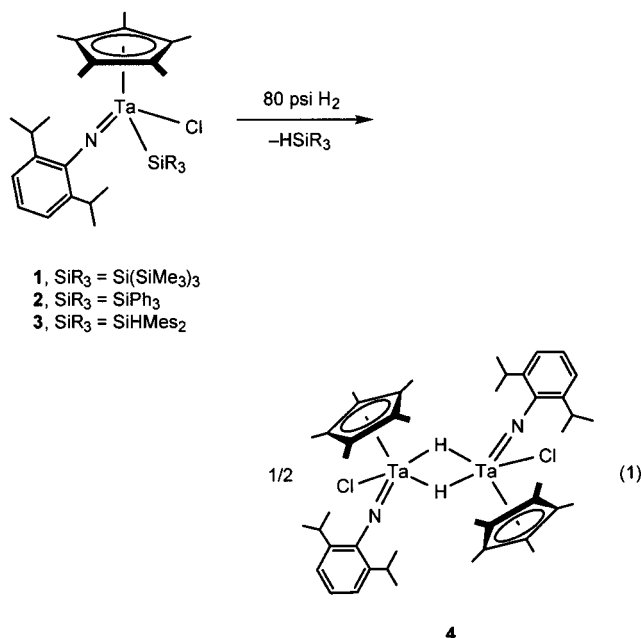
In this account we describe the syntheses, structures, and reactivities of a number of alkyl, silyl, and hydride complexes of tantalum(V), Cp*(DippN=)TaRR' (Cp* = η^5 -C₅Me₅; R = silyl, alkyl; R' = alkyl, hydride), which contain a mixed pentamethylcyclopentadienyl-(aryl)-imido ligand set. Important synthetic targets have been coordinatively unsaturated d^0 silyl hydride complexes, especially since such species have been proposed as intermediates in metal-catalyzed silane dehydropolymerization. Complexes of this type possess two different bonds which readily participate in σ -bond metathesis processes (M–Si and M–H), and perhaps for this reason only a few examples have been reported.^{21–26} Herein we describe an isolable 16-electron tantalum(V) silyl hydride complex and its reaction chemistry.

Results and Discussion

Synthesis and Hydrogenolysis of Silyl Chloride Complexes. The dichloride complex Cp*(DippN=)TaCl₂ (Cp* = η^5 -C₅Me₅; Dipp = 2,6-*i*-Pr₂C₆H₃)^{27,28} provides a convenient starting material for the synthesis of tantalum(V) alkyl and silyl complexes containing a mixed pentamethylcyclopentadienyl-(aryl)imido ligand set. Treatment of Cp*(DippN=)TaCl₂ with (THF)₃LiSi(SiMe₃)₃ (1 equiv) afforded the highly crystalline red complex Cp*(DippN=)Ta[Si(SiMe₃)₃]Cl (**1**) in 80% yield. In the ²⁹Si NMR spectrum of **1**, the Ta-bound silicon appears at –47.8 ppm, and this value is intermediate between those reported for CpCp*Hf[Si(SiMe₃)₃]Cl (–77.9 ppm)²⁹ and (DippN=)₂W[Si(SiMe₃)₃]Cl (–22.9 ppm).¹⁸

Reactions of Cp*(DippN=)TaCl₂ with (THF)₃LiSiPh₃ and (THF)₂LiSiHMe₂ (Mes = 2,4,6-Me₃C₆H₂) provided the analogous silyl chloride complexes Cp*(DippN=)Ta(SiPh₃)Cl (**2**) and Cp*(DippN=)Ta(SiHMe₂)Cl (**3**), respectively. These compounds are difficult to purify due to their high solubility in hydrocarbon solvents. The ²⁹Si NMR resonances for **2** and **3** were found at 51.4 and 17.6 ppm, respectively, and the latter appears as a doublet with ¹J_{SiH} = 163 Hz.

Hydrogenolysis (80 psi, room temperature, 1 h) of hexanes solutions of the silyl chloride complexes **1–3** immediately led to precipitation of the yellow hydrido chloride complex [Cp*(DippN=)TaCl(μ -H)]₂ (**4**), in nearly quantitative yield (eq 1). Complex **4** has poor solubility in most solvents and can be easily isolated from the hydrosilane byproduct by washing with hexanes. The ¹H NMR spectrum of **4** (in dichloromethane-*d*₂) contains a singlet for the bridging hydrides at 7.91 ppm and two sets of isopropyl resonances. The IR spectrum contains a strong, broad band for the bridging hydrides at 1606 cm^{–1} (**4-d**: ν_{TaD} = 1151 cm^{–1}).



Synthesis and Structural Characterization of Silyl Hydride Complexes. The addition of 2 equiv of (THF)₃LiSi(SiMe₃)₃ to a THF slurry of **4** produced a clear yellow solution from which lemon-yellow crystals (**5**, 89% yield) were isolated by crystallization from THF/pentane. The crystals lose solvent after prolonged exposure to vacuum, as evidenced by a color change from yellow to dark red (see below). NMR and elemental analysis characterize complex **5** as an adduct of the desired silyl hydride **6** with 1 equiv of LiCl and 3 equiv of THF. The IR spectrum contains a weak Ta–H stretch at 1805 cm^{–1} (**5-d**: ν_{TaD} = 1282 cm^{–1}). In the ¹H NMR spectrum, the hydride resonance at 12.83 ppm displays distinct ²⁹Si satellites, and the ²⁹Si NMR spectrum contains a doublet for the Ta–Si resonance at –98.4 ppm (J_{SiH} = 31 Hz). The magnitude of this J_{SiH} coupling constant suggests the possibility of a nonclassical

(15) Huber, S. R.; Baldwin, T. C.; Wigley, D. E. *Organometallics* **1993**, *12*, 91.

(16) Gibson, V. C. *J. Chem. Soc., Dalton Trans.* **1994**, 1607.

(17) Gountchev, T. I.; Tilley, T. D. *J. Am. Chem. Soc.* **1997**, *119*, 12831.

(18) Casty, G. L.; Tilley, T. D.; Yap, G. P. A.; Rheingold, A. L. *Organometallics* **1997**, *16*, 4746.

(19) Burckhardt, U.; Casty, G. L.; Tilley, T. D.; Woo, T. K.; Rothlisberger, U. *Organometallics* **2000**, *19*, 3830.

(20) Burckhardt, U.; Tilley, T. D. *J. Am. Chem. Soc.* **1999**, *121*, 6328.

(21) Casty, G. L.; Lugmair, C. G.; Radu, N. S.; Tilley, T. D.; Walzer, J. F.; Zargarian, D. *Organometallics* **1997**, *16*, 8.

(22) Kreutzer, K. A.; Fisher, R. A.; Davis, W. M.; Spaltenstein, E.; Buchwald, S. L. *Organometallics* **1991**, *10*, 4301.

(23) Spaltenstein, E.; Palma, P.; Kreutzer, K. A.; Willoughby, C. A.; Davis, W. M.; Buchwald, S. L. *J. Am. Chem. Soc.* **1994**, *116*, 10308.

(24) Nikonov, G. I.; Mountford, P.; Green, J. C.; Cooke, P. A.; Leech, M. A.; Blake, A. J.; Howard, J. A. K.; Lemenovskii, D. A. *Eur. J. Inorg. Chem.* **2000**, 1917.

(25) Nikonov, G. I. *J. Organomet. Chem.* **2001**, *635*, 24.

(26) Nikonov, G. I.; Mountford, P.; Ignatov, S. K.; Green, J. C.; Leech, M. A.; Kuzmina, L. G.; Razuvaev, A. G.; Rees, N. H.; Blake, A. J.; Howard, J. A. K.; Lemenovskii, D. A. *J. Chem. Soc., Dalton Trans.* **2001**, 2903.

(27) Williams, D. N.; Mitchell, J. P.; Poole, A. D.; Siemeling, U.; Clegg, W.; Hockless, D. C. R.; O'Neill, P. A.; Gibson, V. C. *J. Chem. Soc., Dalton Trans.* **1992**, 739.

(28) Baldwin, T. C.; Huber, S. R.; Bruck, M. A.; Wigley, D. E. *Inorg. Chem.* **1993**, *32*, 5682.

(29) Woo, H.-G.; Heyn, R.; Tilley, T. D. *J. Am. Chem. Soc.* **1992**, *114*, 5698.

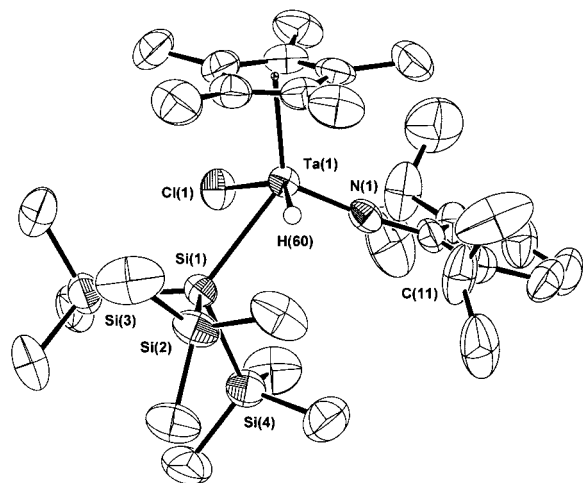
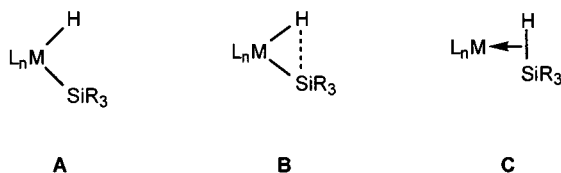


Figure 1. ORTEP diagram of $\{\text{Li}(\text{THF})_4\}\{\text{Cp}^*(\text{DippN}=\text{Ta}(\text{Cl})[\text{Si}(\text{SiMe}_3)_3]\text{H})\cdot(\text{THF})_2$, cation not shown).

Chart 1. Bonding Schemes for Transition Metal Silyl Hydride Complexes



interaction between the hydride and the Ta-bound silicon atom.^{23–25,30–35}

Transition metal complexes containing silyl and hydride ligands adopt different structure types, depending on the degree to which the hydride and silyl groups interact (A–C, Chart 1).³¹ In one limiting case (A), there is no such interaction, as indicated by long H–Si distances and a low J_{SiH} coupling constant (\leq ca. 20 Hz).^{30,36} Another limiting case features strong Si–H bonding, such that the complex is best described as possessing an η^2 -silane ligand (C). Such cases often exhibit relatively high J_{SiH} coupling constants of \geq 50 Hz.^{30–35,37} Other cases appear to be intermediate in character (B), with J_{SiH} values falling in the 20–50 Hz range.^{24,25,30–35} For example, Buchwald's $\text{Cp}_2\text{Ti}(\text{H})(\text{SiHPh}_2)(\text{PMe}_3)$ exhibits a J_{SiH} value of 28 Hz,²³ and Nikonov's $\text{Cp}(\text{DippN}=\text{Ta})(\text{H})(\text{SiMe}_2\text{Cl})(\text{PMe}_3)$, described as possessing a hydride→silicon donor interaction, has a J_{SiH} value of 33 Hz.^{24–26} The observed J_{SiH} coupling constant of 31 Hz for **5** also appears to reflect “intermediate character” of type B.

The molecular structure of **5**·(THF)₂ was determined by X-ray diffraction analysis (Figure 1). Selected bond lengths and angles are listed in Table 1. This ate

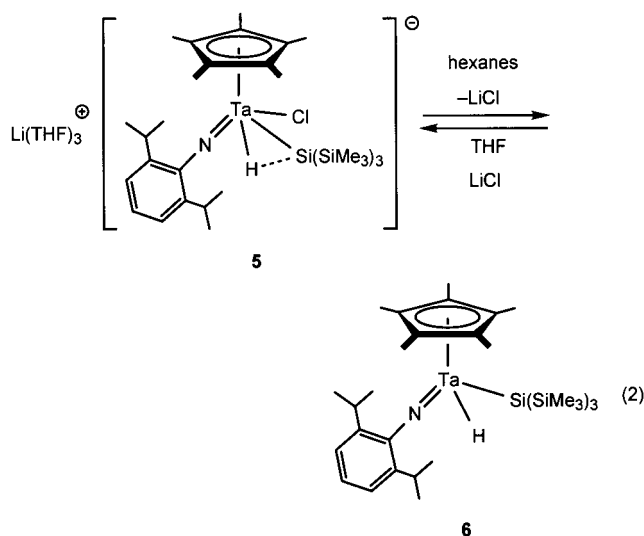
Table 1. Selected Bond Lengths (Å) and Angles (deg) for $\{\text{Li}(\text{THF})_4\}\{\text{Cp}^*(\text{DippN}=\text{Ta}(\text{Cl})[\text{Si}(\text{SiMe}_3)_3]\text{H})\cdot(\text{THF})_2$ ^a

Bond Lengths			
Ta(1)–Cl(1)	2.483(2)	Ta(1)–Si(1)	2.722(3)
Ta(1)–N(1)	1.811(8)	Ta(1)–Cp* _{cent}	2.160
Ta(1)–H(60)	1.67(8)	N(1)–C(11)	1.38(1)
Si(1)–Si(2)	2.345(4)	Si(1)–Si(3)	2.352(5)
	Si(1)–Si(4)		2.351(5)
Bond Angles			
Cl(1)–Ta(1)–Si(1)	79.38(9)	Cl(1)–Ta(1)–N(1)	99.7(2)
Cl(1)–Ta(1)–Cp* _{cent}	106.28(6)	Si(1)–Ta(1)–N(1)	107.7(2)
Si(1)–Ta(1)–Cp* _{cent}	128.63(7)	N(1)–Ta(1)–Cp* _{cent}	120.8(2)
Ta(1)–N(1)–C(11)	174.1(6)	Ta(1)–Si(1)–Si(2)	117.4(1)
Ta(1)–Si(1)–Si(3)	121.8(1)	Ta(1)–Si(1)–Si(4)	107.7(2)
Cl(1)–Ta(1)–H(60)	144(3)	Si(1)–Ta(1)–H(60)	65(3)
N(1)–Ta(1)–H(60)	93(3)	Cp* _{cent} –Ta(1)–H(60)	95(3)

^a Cp*_{cent} represents the average of the *x*, *y*, and *z* coordinates of the η^5 -C₅Me₅ ring carbons.

complex is composed of separated cations and anions, as indicated by a Ta–Cl bond length of 2.483(2) Å and a closest Cl⋯Li distance of 5.286 Å. The slight elongation of the Ta–Si (2.722(3) Å) and Ta–N (1.811(8) Å) bonds compared to those of the corresponding 16-electron complex $\text{Cp}^*(\text{DippN}=\text{Ta}[\text{Si}(\text{SiMe}_3)_3]\text{H}$ (**6**, vide infra) can be rationalized by the higher coordination number for **5**. The hydride ligand, H(60), was located in the Fourier difference map and its position was refined isotropically. The Ta–H distance appears to be somewhat shorter than in other silyl hydride examples, although uncertainties in the hydrogen atom position preclude a meaningful comparison. Further support for a three-center Ta⋯Si⋯H interaction is found in the small values for both the H(60)⋯Si(1) distance (2.51 Å in **5**·(THF)₂, vs 3.39 Å in **6**) and the Si(1)–Ta(1)–H(60) angle (65(3)° in **5**·(THF)₂ vs 97(1)° in **6**).

The addition of hexanes or toluene to **5** immediately generated a deep red solution and a precipitate. After cooling and repeatedly filtering the solution to remove LiCl, the 16-electron silyl hydride complex $\text{Cp}^*(\text{DippN}=\text{Ta}[\text{Si}(\text{SiMe}_3)_3]\text{H}$ (**6**) was isolated as thermally unstable red crystals in 58% yield (eq 2). Despite the



modest isolated yield for **6**, the conversion was quantitative as determined by ¹H NMR spectroscopy. In the ¹H NMR spectrum of **6**, the hydride resonance appears

(30) Schubert, U. *Adv. Organomet. Chem.* **1990**, *30*, 151.

(31) Schubert, U.; Scholz, G.; Müller, J.; Ackermann, K.; Wörle, B.; Stansfield, R. F. D. *J. Organomet. Chem.* **1986**, *306*, 303.

(32) Colomer, E.; Corriu, R. J. P.; Marzin, C.; Vioux, A. *Inorg. Chem.* **1982**, *21*, 368.

(33) Matarasso-Tchiroukhine, E.; Jaouen, G. *Can. J. Chem.* **1988**, *66*, 2157.

(34) Schubert, U.; Wörle, B.; Jandik, P. *Angew. Chem., Int. Ed. Engl.* **1981**, *20*, 695.

(35) Schubert, U.; Müller, J.; Alt, H. G. *Organometallics* **1987**, *6*, 469.

(36) Tilley, T. D. In *Chemistry of Organic Silicon Compounds*; Patai, S., Rappaport, Z., Eds.; Wiley: New York, 1989; p 1415.

(37) Corey, J. Y.; Braddock-Wilking, J. *Chem. Rev.* **1998**, *4*, 1852.

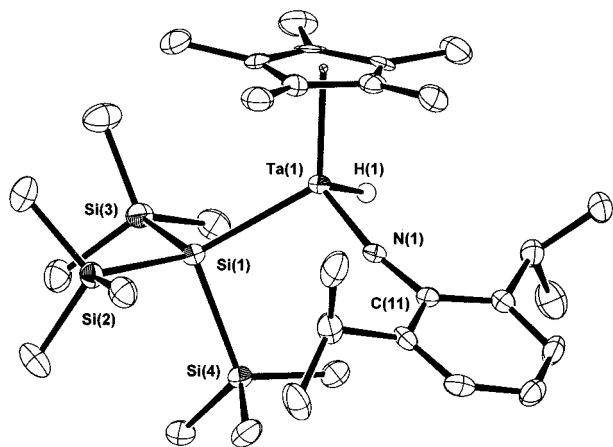


Figure 2. ORTEP diagram of Cp*(DippN=)Ta[Si(SiMe₃)₃]H (**6**).

Table 2. Selected Bond Lengths (Å) and Angles (deg) for Cp*(DippN=)Ta[Si(SiMe₃)₃]H (6**)^a**

Bond Lengths			
Ta(1)–Si(1)	2.689(1)	Ta(1)–N(1)	1.793(4)
Ta(1)–Cp* _{cent}	2.1217(2)	Ta(1)–H(1)	1.77(5)
Si(1)–Si(2)	2.356(2)	Si(1)–Si(3)	2.369(2)
Si(1)–Si(4)	2.376(2)	N(1)–C(11)	1.407(6)
Bond Angles			
Si(1)–Ta(1)–N(1)	106.2(1)	Si(1)–Ta(1)–Cp* _{cent}	122.82(3)
N(1)–Ta(1)–Cp* _{cent}	122.6(1)	Ta(1)–N(1)–C(11)	169.7(3)
Ta(1)–Si(1)–Si(2)	123.36(6)	Ta(1)–Si(1)–Si(3)	116.31(6)
Ta(1)–Si(1)–Si(4)	100.83(6)	Si(1)–Ta(1)–H(1)	97(1)
N(1)–Ta(1)–H(1)	96(1)	Cp* _{cent} –Ta(1)–H(1)	105(1)

^a Cp*_{cent} represents the average of the *x*, *y*, and *z* coordinates of the η⁵-C₅Me₅ ring carbons.

at very low field (21.49 ppm), reflecting the highly electron-deficient character of the metal center. This is also true for the ²⁹Si NMR shift of the central silicon atom, which also appears at unusually low field (–22.9 ppm). A weak IR absorption at 1785 cm^{–1} (**6-d**: ν_{TaD} = 1276 cm^{–1}) is consistent with a terminal Ta–H bond.³⁸ The molecular structure of **6** is shown in Figure 2, and important bond distances and angles are given in Table 2.

Solutions of **6** decompose at room temperature (*t*_{1/2} = 8.5 h in benzene-*d*₆), but can be stored at –30 °C for several days; as a solid, **6** has a longer lifetime. Unlike its hafnocene counterpart CpCp*Hf[Si(SiMe₃)₃]H,²¹ **6** does not appear to be light-sensitive, as decomposition rates are the same in the presence or absence of ambient light. Complex **6** is not stable when isolated, suggesting that THF stabilizes this complex (see below for a discussion of the thermal rearrangement).

Interestingly, the chloride dissociation from **5** is reversible. Solutions of the free silyl hydride **6** in THF-*d*₈ reacted instantly with 1 equiv of LiCl to form **5** (by ¹H NMR spectroscopy). In addition, complex **6** was found to react cleanly with other halides. While THF solutions of **6** decomposed upon addition of CsF, rapid, clean reactions were observed with [NBu₄]Br and [NBu₄]I in THF-*d*₈, to produce the bromide (**7**) and iodide (**8**) complexes, respectively (observed and characterized by NMR spectroscopy). The trend in *J*_{SiH} coupling constants (**5**, 31 Hz; **7**, 33 Hz; **8**, 36 Hz) possibly

reflects a slight steric influence on the degree of Si···H interaction.

Reactions of Cp*(DippN=)Ta[Si(SiMe₃)₃]H (6**).** The relatively rapid decomposition of **6** precludes its large-scale synthesis and storage. However, the chloride adduct **5** can be stored for several weeks, and **6** may be freshly generated before use by dissolving **5** in hexanes, filtering to remove LiCl, and then evaporating the solvent. The reactivity of **6** toward various small molecules is summarized in Scheme 1. Treatment with xylyl (xylyl = 2,6-dimethylphenyl) isocyanide (toluene, room temperature, 6 h) afforded the η²-silaimine insertion product Cp*(DippN=)Ta[η²-C(N-2,6-Me₂C₆H₃)Si(SiMe₃)₃]H (**9**) in 49% yield, although this conversion is quantitative by ¹H NMR spectroscopy. The structural assignment is based upon comparing spectroscopic data with those reported for other early transition metal η²-silaimines.³⁹ Similarly, treatment of **6** with acetonitrile (benzene-*d*₆, room temperature, 5 min, quantitative conversion) gave a thermally unstable product which appears to be the azomethine derivative Cp*(DippN=)Ta[C=N(Me)Si(SiMe₃)₃]H (**10**), on the basis of comparisons with NMR data for known compounds.^{40,41} While both xylyl isocyanide and acetonitrile selectively insert into the Ta–Si bond, acetone inserts into only the Ta–H bond to yield the isopropoxide complex Cp*(DippN=)Ta(OⁱPr)[Si(SiMe₃)₃] (**11**) (benzene-*d*₆, room temperature, 5 min, quantitative conversion; characterized by NMR spectroscopy).

Treatment of complex **6** with ethylene (1 atm, <5 min) or diphenylacetylene (2 equiv, 24 h) resulted in the elimination of HSi(SiMe₃)₃ with formation of the stable, five-membered tantalacycles Cp*(DippN=)Ta[CH₂CH₂–CH₂CH₂] (**12**) and Cp*(DippN=)Ta[CPhCPhCPhCPh] (**13**), respectively. The hydrogenolysis of **6** in hexanes yielded the dimeric dihydride complex [Cp*(DippN=)–TaH(*μ*-H)]₂ (**14**) in 56% yield. Treatment of **6** with dichloromethane gave a mixture of products, the major ones being Cp*(DippN=)TaCl₂, the silyl chloride **1**, and the hydrido chloride **4**. In summary, the reactivity of **6** is similar to that observed for the group 4 silyl hydride complexes CpCp*Hf[Si(SiMe₃)₃]H²¹ and Cp₂Zr(SiPh₃)(PMe₃)H.²²

Thermal Decomposition of Cp*(DippN=)Ta[Si(SiMe₃)₃]H (6**) via C–H Bond Activation.** As mentioned above, solutions of **6** decompose at room temperature (*t*_{1/2} = 8.5 h), as evidenced by a gradual color change from red to yellow. The ¹H NMR spectra indicate that a ca. 2:1 mixture of a new complex (**15**, ca. 60%) and HSi(SiMe₃)₃ (from other decomposition pathways) is formed in various solvents (benzene, hexanes, and diethyl ether), along with small quantities of other products. Attempts to crystallize **15** from the reaction mixture failed. Thus, the structural assignment of **15** is based on spectroscopic data and in particular on ¹H,²⁹Si-HMQ(B)C spectra, which were essential to establish the connectivity of atoms. Complex **15** was determined to be a product of the rearrangement of **6**,

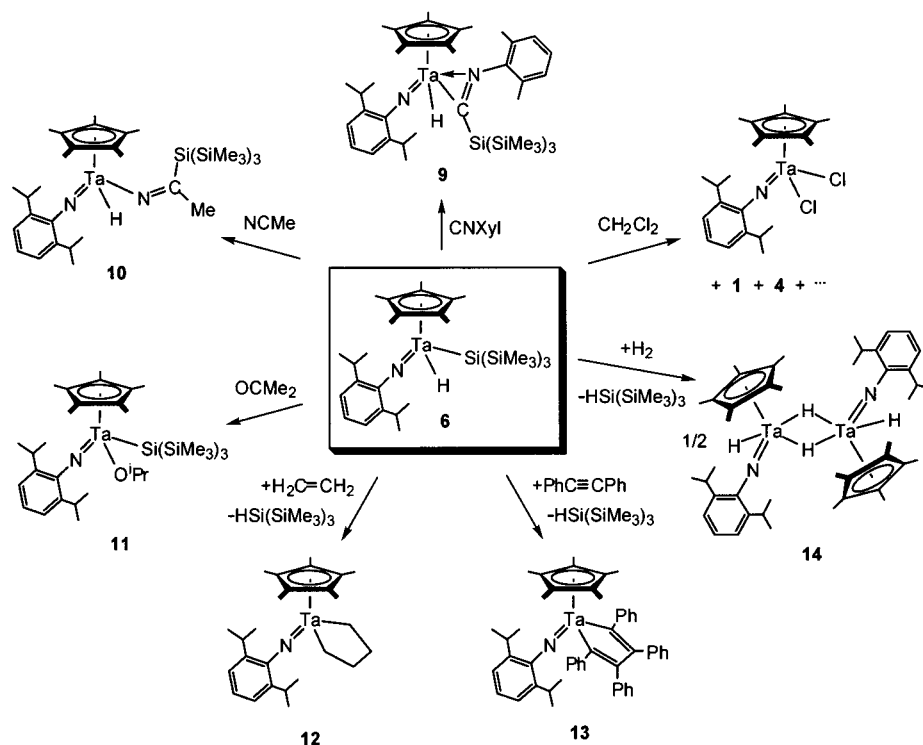
(39) Elsner, F. H.; Tilley, T. D.; Rheingold, A. L.; Geib, S. J. *J. Organomet. Chem.* **1988**, *358*, 169.

(40) Bercaw, J. E.; Davies, D. L.; Wolczanski, P. T. *Organometallics* **1986**, *5*, 443.

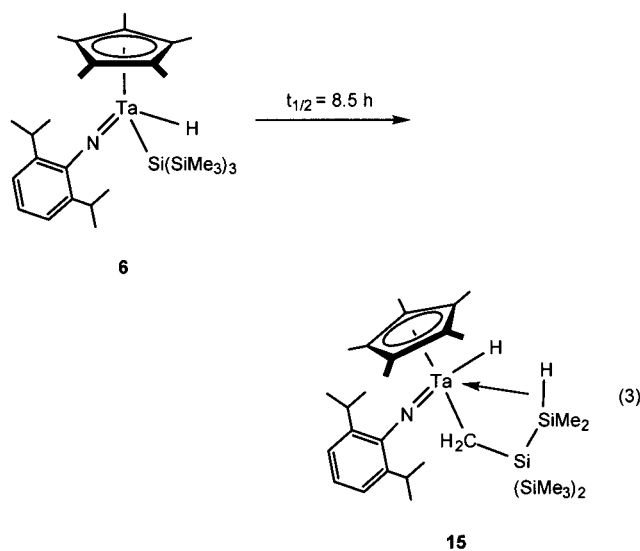
(41) Woo, H.-G.; Tilley, T. D. *J. Organomet. Chem.* **1990**, *393*, C6.

(38) Jiang, Q.; Carroll, P. J.; Berry, D. H. *Organometallics* **1991**, *10*, 3648.

Scheme 1



with the former silyl ligand, $-\text{Si}(\text{SiMe}_3)_3$, being converted to the alkyl ligand $-\text{CH}_2\text{Si}(\text{SiMe}_3)_2\text{SiMe}_2\text{H}$ (eq 3).



The ^1H NMR spectrum of **15** reveals chemical shift values of 9.58 ppm (dd) for the tantalum hydride resonance, 0.70 ppm (ddd) and -0.90 ppm (dd) for the resonances of the diastereotopic methylene hydrogens, and 2.57 ppm (dddq) for the Si–H resonance. The Si–H resonance appears at ca. 2 ppm higher field than expected for a typical Si–H group, suggesting a non-classical (agostic)⁴² interaction of the Si–H unit with the tantalum. Consistent with this hypothesis is the exceptionally large J_{HH} coupling constant of 9 Hz involving the Si–H and Ta–H hydrogens, a value

hardly conceivable for a regular $^5J_{\text{HH}}$ coupling (assignment of J -values confirmed by homonuclear decoupling experiments). A phase-sensitive ^1H NOESY experiment revealed a strong NOE signal correlating Ta–H and Si–H, but no chemical exchange.

The ^{29}Si NMR spectrum of **15** provides further support for the above interpretations. While normal chemical shift values are observed for the ^{29}Si NMR resonances of the $-\text{Si}(\text{SiMe}_3)_2-$ group (-10.5 , -11.1 , and -88.3 ppm), the $-\text{SiMe}_2\text{H}$ resonance is located at -68.9 ppm, >30 ppm upfield from what is expected. The J_{SiH} coupling constant is moderately temperature-dependent (78 Hz at -70 °C, 87 Hz at 25 °C, and 101 Hz at 80 °C) and is about half the magnitude of a normal one-bond J_{SiH} coupling constant, once again suggesting a γ -agostic interaction with the tantalum metal center. The IR spectrum of **15** contains a ν_{SiH} stretch at 1726 cm^{-1} , well below typical values found for normal Si–H bonds (around 2150 cm^{-1}).⁴³ The mass spectrum (EI⁺) of **15** contains a peak at 737 ($[\text{M}]^+ - 2$), which is more intense than the molecular peak at 739 (by a factor of 11), indicating facile loss of H_2 , presumably from the Ta–H and Si–H hydrogens, which are in close contact (as determined by the ^1H NOESY experiment, see above). However, no hydrogen evolution was observed by ^1H NMR spectroscopy on heating the sample in a sealed NMR tube (toluene- d_8 , 90 °C).

All of the above spectroscopic features are in good agreement with those reported for the related zirconium complexes $\text{Cp}_2\text{Zr}(\text{X})(\text{N}^t\text{BuSiMe}_2\text{H})$ ⁴⁴ and $\text{Cp}_2\text{Zr}(\eta^2\text{-RC}\equiv\text{CSiMe}_2\text{H})$,⁴⁵ both of which have been demonstrated to

(43) Corey, J. Y.; Braddock-Wilking, J. *Chem. Rev.* **1999**, *99*, 175.

(44) Procopio, L. J.; Carroll, P. J.; Berry, D. H. *J. Am. Chem. Soc.* **1994**, *116*, 177.

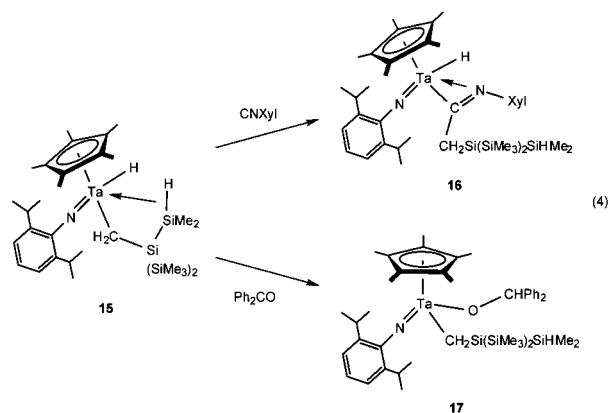
(45) Peulecke, N.; Ohff, A.; Kosse, P.; Tillack, A.; Spannenberg, A.; Kempe, R.; Baumann, W.; Burlakov, V. V.; Rosenthal, U. *Chem. Eur. J.* **1998**, *4*, 1852.

(42) Brookhart, M.; Green, M. L. H. *J. Organomet. Chem.* **1983**, *250*, 395.

exhibit agostic β -Si-H interactions. Consequently, we postulate a cyclic structure for **15** in which the terminal $-Me_2SiH$ group of the polysilyl ligand is coordinated to tantalum (an agostic γ -Si-H interaction). To the best of our knowledge, this coordination mode is unprecedented.³⁷ To confirm the connectivity of the alkyl group, complex **15** was hydrolyzed with H_2O and D_2O and the silane products were analyzed by NMR spectroscopy and GCMS. Spectroscopic data for the principal products are consistent with the formula $Me_2HSi-Si(SiMe_3)_2CH_2-H(D)$ and match recently published data for this silane.⁴⁶

Evaporation of solutions of **15** produced a yellow oil, as did attempts to crystallize the product from pentane and hexamethyldisiloxane (at -30 °C). On standing at room temperature, solutions of **15** completely decompose to a complex mixture of species within ca. one week (1 day at 50 °C). From the complex product mixture, a small amount of a yellow solid separates, which was determined by IR and NMR spectroscopy to be an asymmetric, hydride-bridged dimer, $\{Cp^*(DippN=)Ta[CH_2Si(SiMe_3)_2SiMe_2H]\}(\mu-H)_2\{TaCp^*(=NDipp)H\}$ (**18**), characterized by two bridging hydrides ($\nu_{Ta-(\mu-H)} = 1508$ and 1619 cm^{-1} ; $\delta(Ta-(\mu-H)) = 6.99$ (m) and 6.63 (dd)), a terminal hydride ($\nu_{TaH} = 1794$ cm^{-1} ; $\delta(Ta-H) = 14.93$ (dd)), and an Si-H group ($\nu_{SiH} = 2086$ cm^{-1} ; $\delta(Si-H) = 4.69$ (m)).

Complex **15** readily inserts unsaturated molecules into its Ta-C or Ta-H bonds. In these reactions, the agostic- Me_2SiH group dissociates from the metal center, as indicated by new spectroscopic properties of the $-Me_2SiH$ group. Addition of xylyl isocyanide (1 equiv) to a solution of crude **15** (benzene- d_6 , room temperature, 1 h) produced the dark orange-brown η^2 -imine complex **16**, and the structure shown in eq 4 is based mostly on



spectroscopic data ($\delta(Ta-H) = 10.26$ ppm; $\delta(Si-H) = 3.83$ ppm; $\delta(^{29}Si-H) = -27.2$ ppm, $^1J_{SiH} = 174$ Hz), MS ($[M]^+ = 870$ m/z). This conversion is quantitative (by NMR spectroscopy), but isolation of the pure product was unsuccessful due to its high solubility in hydrocarbon solvents. Similarly, **15** reacted quantitatively with 1 equiv of benzophenone (hexanes, room temperature, 10 s) to produce the alkoxide complex **17**, as indicated by a color change to bright yellow (eq 4). A new SiH resonance is observed in the 1H NMR spectrum at 6.74 ppm, and other NMR data indicate the formation of an alkoxide ligand (for $OCHPh_2$: $\delta(O^{13}CHPh_2) = 89.0$ ppm, $\delta(^{29}Si-H) = -27.4$ ppm, $^1J_{SiH} = 183$ Hz).

(46) Herzog, U.; Roewer, G. *J. Organomet. Chem.* **1997**, *527*, 117.

The mechanism for the formation of **15** is not apparent since no intermediate species could be detected by monitoring the reaction progress by NMR spectroscopy. The only direct information relates to the fate of the hydride ligand. Rearrangement of the deuterium-labeled compound $Cp^*(DippN=)Ta[Si(SiMe_3)_3]D$ (**6-d**) results in deuterium incorporation into only the agostic $-Me_2SiD$ group, and no deuterium is found in the SiH position of the $HSi(SiMe_3)_3$ byproduct. In the final stage of the reaction, some hydrogen scrambling into the $-Me_2SiD$ position is observed, probably due to reaction with the tantalum hydride species. This finding rules out the otherwise plausible possibility of a reductive silane elimination from **6** followed by an oxidative addition of an $-SiMe_3$ group, as the competitive loss of silane would produce $DSi(SiMe_3)_3$. On the basis of the observed $-SiMe_3$ migrations in isomerizations of the coordinatively unsaturated rhodium and iridium polysilyl complexes $(Me_3P)_3M-Si(SiMe_3)_3$,^{47,48} a reaction sequence like the one depicted in Scheme 2 seems possible for the rearrangement of **6** to **15**. Migration of the hydride to the imido nitrogen would create a coordinatively unsaturated Ta(III) amido species in which a series of silylene-generating 1,2- and 1,3-migrations of $SiMe_3$ could take place. Such reactions have been observed for late transition metal silyl complexes.^{36,49-51} Oxidative addition of a C-H bond of a methyl group, followed by α -abstraction of the amido hydrogen by the Ta-bound $SiMe_2$ group, would then produce **15**. However, a gradient-enhanced $^1H, ^{15}N$ -HMQC experiment performed to detect possible tantalum amido species did not show any signals arising from N-H bonds upon monitoring the decomposition of **6** in benzene- d_6 (room temperature). In the absence of further experimental data, alternative mechanisms have to be considered, in particular those involving a concerted double migration at silicon (i.e., a "dyotropic shift").⁵²

Thermal Rearrangement via C-H Bond Activation in a Ta-SiHMe₂ Complex. Starting from $[Cp^*(DippN=)TaCl(\mu-H)]_2$ (**4**), several attempts were made to access silyl hydride complexes with silyl groups other than $-Si(SiMe_3)_3$. Treatment of **4** with $(THF)_3LiSiPh_3$ (2 equiv) in THF (room temperature, 1 h) produced a clear orange solution, from which the chloride-stabilized silyl hydride $\{Li(THF)_3\}\{Cp^*(DippN=)TaCl(SiPh_3)H\}$ (**19**) was isolated by precipitation with pentane in 66% yield. The 1H NMR spectrum of **19** contains broad resonances for the phenyl and isopropyl groups due to hindered rotation, and characteristic silicon satellites were identified for the hydride resonance at 11.97 ppm ($J_{SiH} = 34$ Hz). In contrast to its $-Si(SiMe_3)_3$ analogue **6**, complex **19** does not convert to a free silyl hydride complex when dissolved in hydrocarbons; the chloride remains coordinated. Within 1 day, **19** decomposed to a mixture of unidentified products, none of which possess a Ta-Si bond (by ^{29}Si NMR spectroscopy).

In contrast, treatment of **4** with $(THF)_2LiSiHMe_2$ (2 equiv) in diethyl ether (room temperature, 12 h) pro-

(47) Mitchell, G. P.; Tilley, T. D.; Yap, G. P. A.; Rheingold, A. L. *Organometallics* **1995**, *14*, 5472.

(48) Mitchell, G. P.; Tilley, T. D. *Organometallics* **1996**, *15*, 3477.

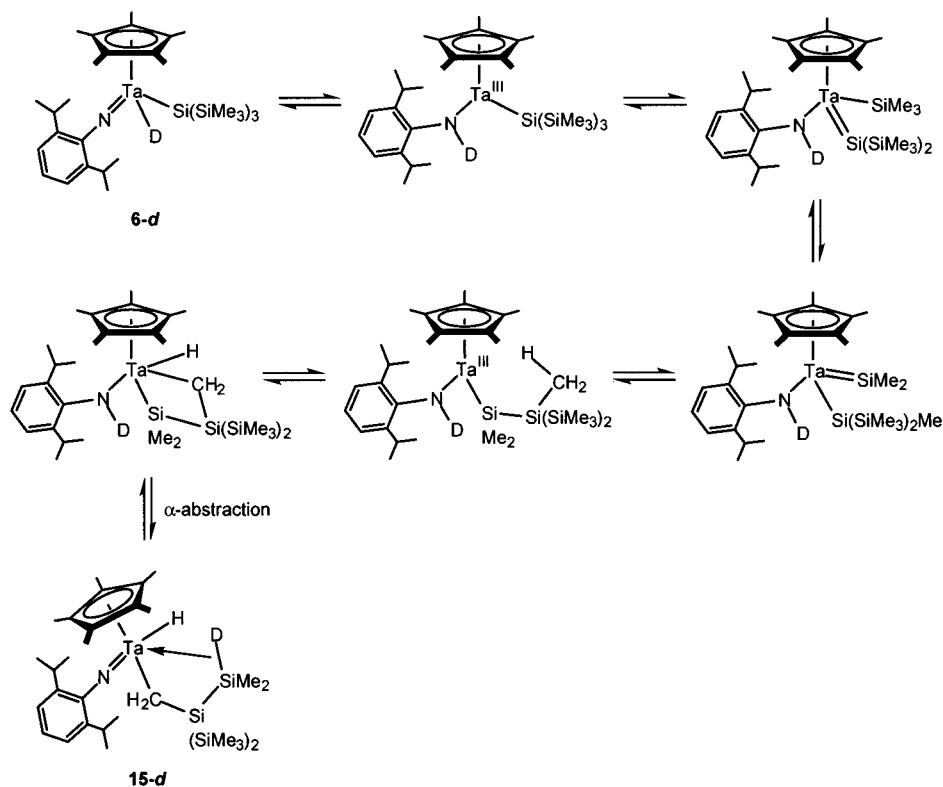
(49) Pannell, K. H.; Sharma, H. K. *Chem. Rev.* **1995**, *95*, 1351.

(50) Schubert, U. *Angew. Chem., Int. Ed. Engl.* **1994**, *33*, 419.

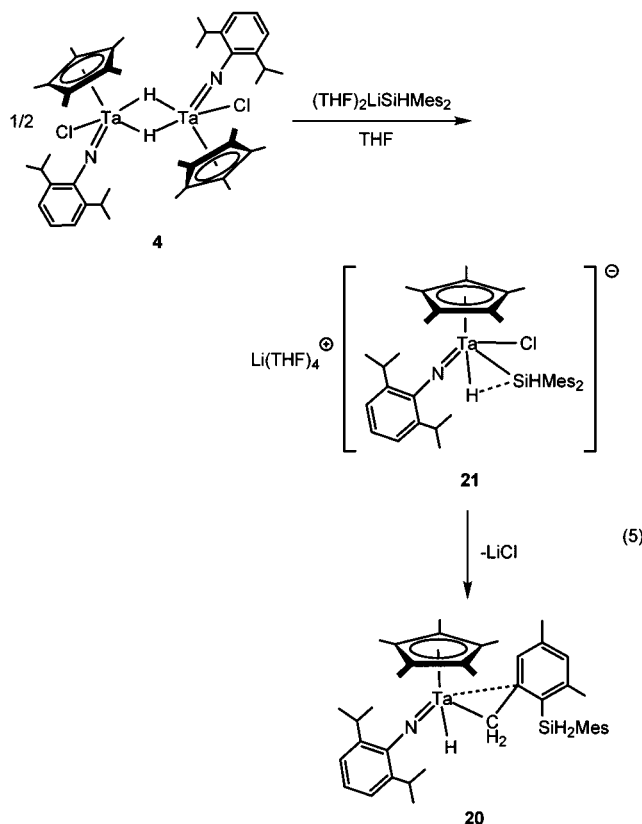
(51) Tilley, T. D. In *The Silicon-Heteroatom Bond*; Patai, S., Rapoport, Z., Eds.; Wiley: New York, 1991; pp 245, 309.

(52) Reetz, M. T. *Adv. Organomet. Chem.* **1977**, *16*, 33.

Scheme 2



duced the hydride complex $\text{Cp}^*(\text{DippN}=\text{Ta}[\eta^2\text{-CH}_2(2\text{-SiH}_2\text{Mes-3,5-Me}_2\text{C}_6\text{H}_2)]\text{H})\text{H}$ (**20**), which was isolated from hexanes as pale yellow crystals in 7% yield (eq 5). This



conversion is quantitative (by NMR spectroscopy), but the high solubility of the product hindered attempts to isolate large amounts of the complex by crystallization.

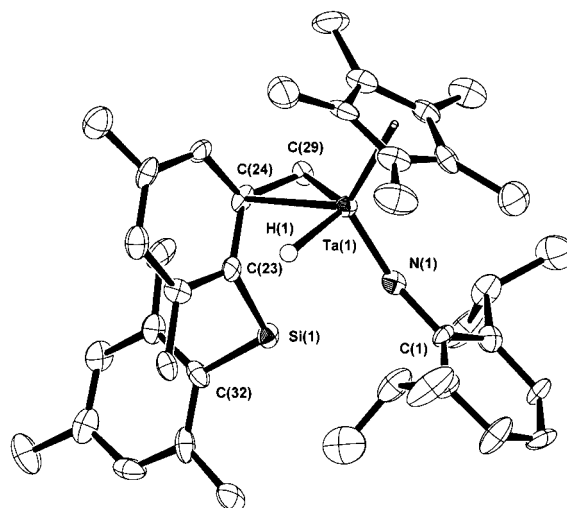


Figure 3. ORTEP diagram of $\text{Cp}^*(\text{DippN}=\text{Ta}[\eta^2\text{-CH}_2(3,5\text{-Me}_2\text{-2-SiH}_2\text{Mes})\text{C}_6\text{H}_2])\text{H}$ (**20**).

The ¹H NMR spectrum of **20** contains a singlet at 8.62 ppm attributed to the Ta–H resonance and two doublets for the geminal Si–H hydrogens at 5.14 and 5.03 ppm (²J_{HH} = 4 Hz). The presence of inequivalent mesityl methyl groups and a diastereotopic methylene group (doublets at 3.60 and 1.90 ppm, ²J_{HH} = 7.3 Hz) are consistent with activation of a methyl group on the mesityl ring.

The structure of **20** was determined by X-ray crystallography (Figure 3), and selected bond distances and angles are listed in Table 3. A peak found in the difference Fourier map is consistent with the position of a tantalum hydride (Ta(1)–H(1) = 1.795 Å), but the refinement did not include this atom. The hydrogens on C(29) and Si(1) were located in the difference Fourier

Table 3. Selected Bond Lengths (Å) and Angles (deg) for Cp*(DippN=)Ta[η²-CH₂(2-SiH₂Mes-3,5-Me₂C₆H₂)]H (20)^a

Bond Lengths			
Ta(1)–N(1)	1.801(8)	Ta(1)–C(24)	2.426(8)
Ta(1)–C(29)	2.244(9)	Ta(1)–Cp* _{cent}	2.1303(4)
N(1)–C(1)	1.41(1)	Ta(1)–H(1)	1.795
Si(1)–C(23)	1.88(1)	Si(1)–C(32)	1.87(1)
Bond Angles			
N(1)–Ta(1)–C(24)	111.3(3)	N(1)–Ta(1)–C(29)	103.5(3)
N(1)–Ta(1)–Cp* _{cent}	120.3(2)	C(24)–Ta(1)–C(29)	35.8(3)
C(24)–Ta(1)–Cp* _{cent}	125.7(2)	C(29)–Ta(1)–Cp* _{cent}	112.0(2)
Ta(1)–N(1)–C(1)	164.4(6)	Ta(1)–C(24)–C(29)	65.2(5)
N(1)–Ta(1)–H(1)	92.37	C(24)–Ta(1)–H(1)	79.26
C(29)–Ta(1)–H(1)	114.72	Cp* _{cent} –Ta(1)–H(1)	112.51

^a Cp*_{cent} represents the average of the *x*, *y*, and *z* coordinates of the η⁵-C₅Me₅ ring carbons.

map but placed in calculated positions. The alkyl ligand is bound to the metal through asymmetric η²-coordination of C(24) and C(29) with tantalum–carbon bond distances of 2.426(8) and 2.244(9) Å, respectively.

The silyl hydride complex generated upon loss of LiCl (analogous to the formation of **6** from **5**) is apparently not stable, giving rise to **20**. Monitoring the reaction of **4** and (THF)₂LiSiHMe₂ by ¹H NMR spectroscopy as the chilled (–30 °C) THF-*d*₈ reaction mixture was slowly warmed to room temperature in the NMR probe revealed the initial formation of the silyl hydride complex {Li(THF)_{*n*}}{Cp*(DippN=)TaCl[SiHMe₂]H} (**21**), with δ(Ta–H) = 12.26 ppm and diagnostic ²⁹Si satellites (*J*_{SiH} = 33 Hz). Within 5 min, **21** is completely converted to **20** and several unidentified byproducts (the reaction is not as clean as in diethyl ether). A likely mechanism for the formation of **20** involves reductive elimination of H₂SiMe₂, followed by oxidative addition of a C–H bond of H₂SiMe₂ to the Ta^{III} center of Cp*(DippN=)Ta to produce the observed product. However, alternative mechanisms involving an intramolecular σ-bond metathesis pathway or an initial hydride shift to nitrogen (vide supra) cannot be ruled out. Treatment of deuterium-labeled **4-d** with (THF)₂LiSiHMe₂ gave inconclusive results regarding deuterium incorporation and did not provide evidence to eliminate any of the above possibilities.

The pairwise conversion of Ta–Si and C–H bonds to Ta–C and Si–H bonds seems to be a generally favorable process, given that both tantalum silyl hydrides **6** and **21** intramolecularly rearrange to tantalum alkyl hydrides. However, no evidence has been found for *inter*-molecular C–H bond activation processes (e.g., the activation of solvent). For example, use of mesitylene as the solvent for the decomposition of **5** to **15** and HSi(SiMe₃)₃ did not result in any visible mesitylene activation or change in the product distribution.

Synthesis and Reactivity of Alkyl Silyl and Alkyl Hydride Complexes. The Cp*(DippN=)Ta fragment was also found to support alkyl hydride complexes of the type Cp*(DippN=)Ta(R)H (R = Me, CH₂CMe₃). However, an initial attempt to prepare a methyl hydride complex from **4** and MeMgBr (2 equiv) was unsuccessful. Surprisingly, only the dimethyl derivative Cp*(DippN=)TaMe₂ (**22**) was formed in this reaction, instead of the expected methyl hydride complex. Therefore, efforts were focused on synthesis of the methyl hydride via hydrogenolysis of the methyl silyl complex

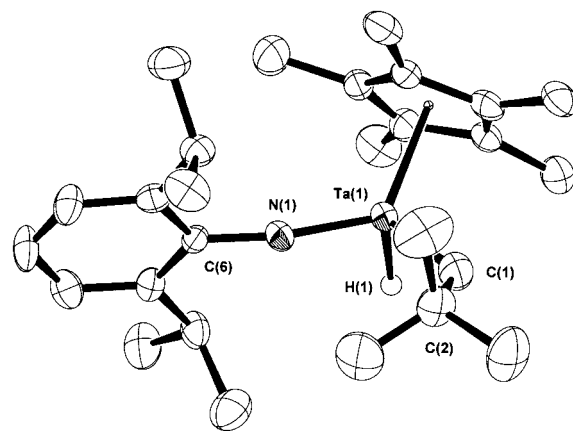


Figure 4. ORTEP diagram of Cp*(DippN=)Ta(CH₂CMe₃)H (**26**).

Cp*(DippN=)Ta[Si(SiMe₃)₃]Me (**23**), prepared by treating **1** with MeMgBr (1 equiv) in diethyl ether (55% yield). At room temperature in benzene-*d*₆ solution, **23** decomposed to Si(SiMe₃)₄ and **22** (over 36 h). Complex **23** reacted quantitatively with carbon monoxide (1 atm, benzene-*d*₆, 1 h) to give the stable η²-silaacyl complex Cp*(DippN=)Ta[η²-COSi(SiMe₃)₃]Me (**24**), identified by the characteristic low-field ¹³C NMR shift of the carbonyl resonance (δ = 408.6 ppm) and the very low carbonyl stretching frequency (ν_{CO} = 1421 cm^{–1}).³⁹ Hydrogenolysis of **23** (1 atm of H₂) afforded the desired methyl hydride [Cp*(DippN=)TaMe(μ-H)]₂ (**25**) in 94% yield (quantitative conversion by ¹H NMR spectroscopy); at 40 psi H₂, only decomposition products were observed. A strong ν_{Ta–(μ-H)} stretch at 1595 cm^{–1} and poor solubility in hydrocarbon solvents support the formulation of complex **25** as a dimer containing bridging hydride ligands.³⁸

The analogous neopentyl hydride complex Cp*(DippN=)Ta(CH₂CMe₃)H (**26**) was obtained directly from **4** and neopentylmagnesium chloride (2 equiv) in 66% yield. Complex **26** is stable in solution at temperatures up to approximately 50 °C (benzene-*d*₆), but rapidly decomposes at higher temperatures to give neopentane, H₂, and many unidentified species (by ¹H NMR spectroscopy). The ¹H NMR spectrum of **26** contains a doublet at 15.09 ppm for the hydride ligand, and the two signals for the diastereotopic methylene hydrogens are separated by more than 5 ppm (doublet at 3.04 ppm, doublet of doublets at –2.21 ppm). The latter, upfield chemical shift indicates that one of the methylene hydrogens possesses some agostic character. This assumption is further supported by the unusually low-field methylene resonance (127.0 ppm) and the low ¹*J*_{CH} value associated with the hydrogen resonating at –2.21 ppm (89 Hz), which is typical for an agostic structure (¹*J*_{CH} = 115 Hz for the other methylene hydrogen).⁴²

An ORTEP drawing of **26** is shown in Figure 4, and selected bond distances and angles are given in Table 4. The hydride, H(1), was located in the difference Fourier map but not included in the refinement. The hydrogens bonded to the Ta-bound carbon, C(1), could not be located from the difference Fourier map and were refined in geometrically calculated positions. The Ta(1)–C(1)–C(2) angle of 134.0(5)° is somewhat large, as might be expected for an α-agostic C–H interaction.

Table 4. Selected Bond Lengths (Å) and Angles (deg) for Cp*(DippN=)Ta(CH₂CMe₃)H (26)^a

Bond Lengths			
Ta(1)–N(1)	1.791(4)	Ta(1)–C(1)	2.121(7)
Ta(1)–Cp* _{cent}	2.1215(2)	Ta(1)–H(1)	1.660
N(1)–C(6)	1.403(7)	C(1)–C(2)	1.539(9)
Bond Angles			
N(1)–Ta(1)–C(1)	107.9(2)	N(1)–Ta(1)–Cp* _{cent}	124.0(1)
C(1)–Ta(1)–Cp* _{cent}	116.2(2)	Ta(1)–N(1)–C(6)	168.6(4)
Ta(1)–C(1)–C(2)	134.0(5)	N(1)–Ta(1)–H(1)	95.61
C(1)–Ta(1)–H(1)	101.55	Cp* _{cent} –Ta(1)–H(1)	106.92

^a Cp*_{cent} represents the average of the *x*, *y*, and *z* coordinates of the η⁵-C₅Me₅ ring carbons.

For comparison, the neopentyl molybdenum complex (DippN=)₂Mo[Si(SiMe₃)₃]CH₂CMe₃, characterized as possessing an α-H agostic interaction, exhibits a Mo(1)–C(1)–C(2) bond angle of 136.6(2)°.¹⁸

To investigate the possibility of reductive elimination/oxidative addition equilibria involving the reversible formation of neopentane, the deuteride Cp*(DippN=)-Ta(CH₂CMe₃)D (**26-d**) was prepared and studied. Benzene-*d*₆ solutions of **26-d** did not exhibit deuterium scrambling after 7 days at room temperature. At higher temperatures, decomposition was fast with only slight (<10%) deuterium incorporation into liberated neopentane and the methylene positions of the intact complex (by ¹H and ²H NMR spectroscopy). However, NMR spectra of **26-d** which had been stored as a crystalline material for four months at room temperature exhibited ca. 50% hydrogen incorporation into the deuteride position and deuterium scrambling mainly into the CMe₃ and ⁱPr (methyl and methine) positions of the ligands. This indicates that various C–H addition and elimination reactions indeed take place, but they are slow and not very selective.

Conclusions

The results described here demonstrate that the Cp*(DippN=)Ta fragment supports stable complexes containing reactive M–R (R = H, silyl) σ-bonds. This system represents some of the few complexes that contain both imido ligands and highly reactive σ-bonds and provides further examples of novel σ-bond metathesis reactivity for d⁰ imido complexes. One of the first tantalum complexes of this type was Bercaw's imido hydride Cp*Ta(=NPh)H, which is formed by an α-migration in the amido complex Cp*₂TaNHPh.^{53–55} Xue and co-workers have reported imido silyl complexes of the type (Me₃SiN=)[(Me₃Si)₂N]Ta[Si(^tBu)Ph₂]X (X = Si(^tBu)Ph₂, NMe₂), which are being studied as precursors for the preparation of Ta–Si–N ternary materials.⁵⁶ More recently, Nikonov has described the silyl hydride Cp(DippN=)Ta(H)(SiMe₂Cl)(PMe₃), which contains a three-center Si⋯Ta⋯H interaction.^{24–26}

We are interested in possible σ-bond metathesis reactions of d⁰ imido complexes. Of course, for early metal imido complexes possessing reactive hydride and/

or silyl ligands, possible alternate reaction pathways include migration of a group to the imido nitrogen atom and concerted addition of a substrate (e.g., H₂ or a hydrosilane) across the M=N double bond. We have recently reported the reaction of Cp*(DippN=)Ta[Si(SiMe₃)₃]H (**6**) with PhSiH₃ by way of Si–N coupling to form two dimeric products with bridging silanimine ligands.¹⁹ The major product, Cp*₂Ta₂H₂(μ-DippNSiHPh)₂, is a dimer resulting from the net addition of PhSiH₃ across the Ta=N double bond. While the mechanism for the formation of this product is uncertain, one possible pathway involves the introduction of a –SiH₂-Ph ligand, which can then migrate to the imido nitrogen atom. For chelating imido-amido complexes of the type

Cp*Ta[=N(C₆H₃Me)₂]NSiMe₃]Me, silanes were observed to add across the Ta=N double bond via an intermediate pentacoordinate silicon species.¹⁷

The silyl hydride complex **6** is remarkably electrophilic, as indicated by its reversible binding of halides (Cl, Br, I) to form ate complexes of the type {Cp*(DippN=)Ta(X)[Si(SiMe₃)₃]H}[–] (**5**, **7**, and **8**, respectively). Interestingly, the formation of these species is accompanied by intramolecular couplings of the silyl and hydride ligands to give σ-complexes with significant Si⋯H interactions. This halide binding provides an unusual example of an observed, reversible Si–H bond-making/bond-breaking reaction at a metal center. These Si⋯H interactions are characterized by *J*_{SiH} coupling constants (31–36 Hz) that are intermediate between *J*_{SiH} values reported for silyl hydride complexes and silane complexes with the strongest Si–H interactions.^{24–26,30–35} It is becoming increasingly clear that interactions of this type are common in metal silicon chemistry, in particular for the early transition metals.²⁵

Thermal decomposition of **6** at room temperature (*t*_{1/2} = 8.5 h) gives the rearrangement product Cp*(DippN=)Ta[CH₂Si(SiMe₃)₂SiMe₂H]H (**15**), which contains an unusual γ-agostic Si–H interaction with the metal center. This rearrangement involves an interesting series of Si–Si and Si–C bond-breaking/bond-making steps and C–H bond activation. This process may be compared to the thermal degradation of (DippN=)₂Mo[Si(SiMe₃)₃]H, generated by the reaction of (DippN=)₂Mo[Si(SiMe₃)₃]CH₂CMe₃ with H₂, which decomposes by the elimination of HSiMe₃ (1.8 equiv), presumably via molybdenum silylene complexes such as (DippN=)₂Mo=Si(SiMe₃)₂.¹⁸ Thus, despite the apparent potential for such 1,2-eliminations to occur in d⁰ imido silyl hydride complexes of this type, this is not observed in the Ta system described here, which in contrast features Si–C and C–H bond cleavages. A C–H bond cleavage is also observed in the room-temperature decomposition of {Li(THF)_{*n*}}–{Cp*(DippN=)TaCl[SiH(2,4,6-Me₃C₆H₂)₂]H} (**21**) to Cp*(DippN=)Ta[η²-CH₂(2-SiH₂Mes-3,5-Me₂C₆H₂)]H (**20**), presumably via the silyl hydride intermediate Cp*(DippN=)Ta[SiH(2,4,6-Me₃C₆H₂)₂]H.

In summary, the observed reaction chemistry suggests that new stoichiometric and catalytic processes involving bond-making/bond-breaking steps might be based on silyl and/or hydride complexes containing d⁰ imido fragments. Current research efforts are directed toward the development of such processes with sterically

(53) Antonelli, D. M.; Schaefer, W. P.; Parkin, G.; Bercaw, J. E. *J. Organomet. Chem.* **1993**, *462*, 213.

(54) Blake, R. E.; Antonelli, D. M.; Henling, L. M.; Schaefer, W. P.; Hardcastle, K. I.; Bercaw, J. E. *Organometallics* **1998**, *17*, 718.

(55) Parkin, G.; van Asselt, A.; Leahy, D. J.; Whinnery, L.; Hua, N. G.; Quan, R. W.; Henling, L. M.; Schaefer, W. P.; Santarsiero, B. D.; Bercaw, J. E. *Inorg. Chem.* **1992**, *31*, 82.

(56) Wu, Z.; Xue, Z. *Organometallics* **2000**, *19*, 4191.

demanding imido ligands that support monomeric silyl hydride derivatives.

Experimental Procedures

General Procedures. All experiments were conducted under a nitrogen atmosphere using standard Schlenk techniques or in a Vacuum Atmospheres drybox unless otherwise noted. Dry, oxygen-free solvents were used unless otherwise indicated. Olefin impurities were removed from pentane by treatment with concentrated H₂SO₄, 0.5 N KMnO₄ in 3 M H₂SO₄, and saturated NaHCO₃. Pentane was then dried over MgSO₄, stored over activated 4 Å molecular sieves, and distilled from potassium benzophenone ketyl under a nitrogen atmosphere. Thiophene impurities were removed from benzene and toluene by treatment with H₂SO₄ and saturated NaHCO₃. Benzene and toluene were then dried over MgSO₄ and distilled from potassium under a nitrogen atmosphere. Diethyl ether, THF, and hexanes were distilled from sodium benzophenone ketyl under a nitrogen atmosphere, and dichloromethane was distilled from CaH₂ under a nitrogen atmosphere. Benzene-*d*₆, toluene-*d*₈, and THF-*d*₈ were purified and dried by vacuum distillation from sodium/potassium alloy.

All chemicals were purchased from Aldrich or Fluka and used without further purification unless otherwise indicated. Commercial silanes were dried over 4 Å molecular sieves and distilled prior to use. Carbon monoxide was purchased from Scott Specialty Gases, hydrogen was purchased from Praxair, and deuterium was purchased from Airgas. The compounds Cp*TaCl₄,^{57–60} DippNH(SiMe₃) (Dipp = 2,6-ⁱPr₂C₆H₃),⁶¹ Cp*(DippN=)TaCl₂,^{27,28} (THF)₃LiSi(SiMe₃)₃,⁶² (THF)₃LiSiPh₃,^{63,64} and (THF)₂LiSiHMes₂⁶⁵ were prepared as reported in the literature. Elemental analyses were performed by the College of Chemistry Microanalytical Laboratory at the University of California, Berkeley. Mass spectra (EI⁺) were recorded on a Micromass VG ProSpec instrument (ionization energy: 70 eV). GCMS spectra were measured on a HP 6890 GC instrument equipped with a HP 5973 MS detector. Infrared spectra were recorded on a Mattson FTIR 3000 instrument, as KBr pellets (solids) or as a thin film between KBr plates (oils).

NMR Measurements. Routine ¹H, ²H, and ¹³C NMR spectra were recorded at 298 K on Bruker AMX-300 and AMX-400 spectrometers (fields and solvents specified). All other spectra were measured at 298 K on a Bruker DRX-500 instrument equipped with a 5 mm broad band probe and operating at 500.13 MHz (¹H), 194.37 MHz (⁷Li), 125.77 MHz (¹³C), 99.36 MHz (²⁹Si), or 202.45 MHz (³¹P). Chemical shifts are reported in ppm downfield from internal SiMe₄ (¹H/²H, ¹³C, ²⁹Si) and external 10% aqueous LiCl (⁷Li) and 85% H₃PO₄ (³¹P). Coupling constants are given in Hz. For ¹H NOESY spectra, a mixing time of 1.0 s was applied. ¹H, ¹³C-HMQC spectra were recorded as 2048 × 256 files using a BIRD sequence [$\pi/2(^1\text{H}) = 14.0 \mu\text{s}$; $\pi/2(^{13}\text{C}) = 6.4 \mu\text{s}$]. ²⁹Si NMR spectra were obtained using a refocused INEPT pulse sequence with or without ¹H decoupling; delays were optimized for $J_{\text{SiH}} = 6.4 \text{ Hz}$ [$\pi/2(^1\text{H}) = 14.0 \mu\text{s}$; $\pi/2(^{29}\text{Si}) = 6.6 \mu\text{s}$]. ¹H, ²⁹Si-HMQC(B)C spectra were

acquired as 2048 × 128 files with 16 transients accumulated per T_1 increment and were optimized for an assumed 4 Hz (125 ms) long-range J_{SiH} . The ¹H, ¹⁵N-HMQC experiment for compound **15** was carried out with a gradient (TBI) probe operating at 500.13 MHz (¹H) and 50.69 MHz (¹⁵N), using the inv4gp pulse sequence with a gradient pulse ratio of 70:30:50, a gradient pulse length of 1 ms, and a gradient pulse recovery delay of 200 μs ; the spectrum was optimized for an assumed 80 Hz (6.3 ms) ¹ J_{NH} . Bruker XWINNMR software (ver. 2.1) was used for all NMR data processing.

Cp*(DippN=)Ta[Si(SiMe₃)₃]Cl (1). A solution of Cp*(DippN=)TaCl₂ (3.92 g, 6.97 mmol) and (THF)₃LiSi(SiMe₃)₃ (3.78 g, 8.03 mmol) in cold (−50 °C) diethyl ether (60 mL) was allowed to warm to room temperature and was then stirred for 12 h. The ether was removed in vacuo, the crystalline residue was extracted four times with a total of 80 mL of hexanes, and the combined extracts were filtered. The resulting solution was concentrated to ca. 50 mL and cooled to −25 °C to produce three crops of dark red crystals of **1** (4.33 g, 80%). ¹H NMR (400 MHz, benzene-*d*₆): δ 7.18 (d, 2 H, *m*-Ar-H, $J = 8$), 6.90 (t, 1 H, *p*-Ar-H, $J = 8$), 3.89 (septet, 1 H, ⁱPr-H, $J = 7$), 3.55 (septet, 1 H, ⁱPr-H, $J = 7$), 1.96 (s, 15 H, C₅Me₅), 1.41, 1.31 (2 × d, 2 × 3 H, ⁱPr-Me, $J = 7$), 1.40, 1.21 (2 × d, 2 × 3 H, ⁱPr-Me, $J = 7$), 0.46 (s, 27 H, Si(SiMe₃)₃). ¹³C{¹H} NMR (100 MHz, benzene-*d*₆): δ 150.1, 148.0, 145.2 (Ar C), 125.3, 123.8, 123.4 (Ar CH), 120.5 (C₅Me₅), 28.2, 27.3, 27.1, 26.4, 25.7, 24.5 (ⁱPr), 12.9 (C₅Me₅), 6.1 (Si(SiMe₃)₃). ²⁹Si{¹H} NMR (99 MHz, benzene-*d*₆): δ −3.4 (Si(SiMe₃)₃), −47.8 (Si(SiMe₃)₃). Anal. Calcd for C₃₁H₅₉ClNSi₄Ta (774.56): C, 48.07; H, 7.68; N, 1.81. Found: C, 48.01; H, 7.84; N, 1.76.

Cp*(DippN=)Ta(SiPh₃)Cl (2). A solution of Cp*(DippN=)TaCl₂ (1.34 g, 2.38 mmol) and (THF)₃LiSiPh₃ (1.7 g, 0.38 mmol) in diethyl ether (40 mL) was stirred at room temperature for 1.5 h. The diethyl ether was removed in vacuo, and the oily residue was then extracted into pentane (4 × 20 mL). The combined extracts were concentrated to ca. 20 mL and cooled to −25 °C to produce **2** in two crops as a dark red foam (1.49 g), which could not be completely separated from silane impurities. ¹H NMR (500 MHz, benzene-*d*₆): δ 7.80 (br m, 6 H, *o*-Ph-H), 7.22–6.99 (m, 11 Ar-H), 6.91 (m, 1 H, *p*-Ar-H), 3.55 (septet, 2 H, ⁱPr-H, $J = 7$), 1.83 (s, 15 H, C₅Me₅), 1.27 (d, 6 H, ⁱPr-Me, $J = 7$), 1.04 (br d, 6 H, ⁱPr-Me, $J = 7$). ¹³C{¹H} NMR (126 MHz, benzene-*d*₆): δ 150.1, 145.7 (Ar C), 139.2 (*o*-Ph CH), 128.8, 128.3, 125.1, 123.1 (Ar CH), 120.6 (C₅Me₅), 28.6 (br, ⁱPr CH), 25.4, 24.1 (br, ⁱPr Me), 12.1 (C₅Me₅). ²⁹Si{¹H} NMR (99 MHz, benzene-*d*₆): δ 51.4. MS: m/z 785 (24, [M]⁺), 561 (7), 259 (100, [SiPh₃]⁺), 182 (32, [SiPh₂]⁺), 105 (7, [SiPh]⁺).

Cp*(DippN=)Ta[SiH(2,4,6-Me₃C₆H₂)₂]Cl (3). A solution of Cp*(DippN=)TaCl₂ (1.00 g, 1.78 mmol) and (THF)₂LiSiHMes₂ (0.93 g, 2.2 mmol) in diethyl ether (30 mL) was stirred at room temperature for 4 h. The diethyl ether was removed in vacuo, and the resulting oily residue was extracted into pentane (3 × 15 mL). The extracts were concentrated and cooled to −30 °C to afford two crops of **3** as orange-red crystals (1.09 g, 77%). ¹H NMR (500 MHz, benzene-*d*₆): δ 7.10 (d, 2 H, *m*-Ar-H, $J = 10$), 6.83 (t, 1 H, *p*-Ar-H, $J = 10$), 6.78, 6.66 (2 × s, 2 × 2 Mes-H), 6.66 (s, 1 H, Si-H), 3.72 (sept, 2 H, ⁱPr-H, $J = 7$), 2.89, 2.68 (2 × s, 2 × 6 H, *o*-Mes-Me), 2.17, 2.01 (2 × s, 2 × 3 H, *p*-Mes-Me), 1.85 (s, 15 H, C₅Me₅), 1.35 (d, 6 H, ⁱPr-Me, $J = 7$), 1.04 (br d, 6 H, ⁱPr-Me, $J = 7$). ¹³C{¹H} NMR (126 MHz, benzene-*d*₆): δ 149.3, 146.4, 146.0, 144.9, 139.8, 139.4, 138.8, 129.5, 128.0 (Ar C), 129.7, 129.3 (Mes CH), 125.3, 123.0 (Ar CH), 120.7 (C₅Me₅), 28.2, 25.9 (*o*-Mes Me), 28.0 (ⁱPr CH), 25.7, 24.7 (ⁱPr Me), 21.4, 21.3 (*p*-Mes Me), 11.9 (C₅Me₅). ²⁹Si NMR (99 MHz, benzene-*d*₆): δ 17.6 (d, ¹ $J_{\text{SiH}} = 163$). IR (KBr, cm^{−1}): 2097 (m, ν_{SiH}). MS: m/z 793 (2, [M]⁺), 702 (7), 561 (40), 546 (9), 268 (73, [H₂SiMes₂]⁺), 253 (12), 177 (8), 162 (14), 148 (100, [HSiMes]⁺), 133 (30), 120 (31), 105 (11). Anal. Calcd for C₄₀H₅₅-CINSiTa (794.37): C, 60.48; H, 6.98; N, 1.76. Found: C, 60.40; H, 7.28; N, 1.83.

(57) Sanner, R. D.; Carter, S. T.; Bruton, W. J. *J. Organomet. Chem.* **1982**, *240*, 157.

(58) Gibson, V. C.; Bercaw, J. E.; Bruton, W. J.; Sanner, R. D. *Organometallics* **1986**, *5*, 976.

(59) Yasuda, H.; Okamoto, T.; Nakamura, A. In *Organometallic Syntheses*; King, R. B., Eisch, J. J., Eds.; Elsevier: Amsterdam, 1988; Vol. 4, p 20.

(60) Okamoto, T.; Yasuda, H.; Nakamura, A.; Kai, Y.; Kaneshida, N.; Kasai, N. *Organometallics* **1988**, *7*, 2266.

(61) Chao, Y.-W.; Wexler, P. A.; Wigley, D. E. *Inorg. Chem.* **1989**, *28*, 3860.

(62) Gutekunst, G.; Brook, A. G. *J. Organomet. Chem.* **1982**, *225*, 1.

(63) Olah, G. A.; Hunadi, R. J. *J. Am. Chem. Soc.* **1980**, *102*, 6989.

(64) Dias, H. V. R.; Olmstead, M. M.; Ruhlandt-Senge, K.; Power, P. P. *J. Organomet. Chem.* **1993**, *462*, 1.

(65) Weidenbruch, M.; Kramer, K.; Pohl, S.; Saak, W. *J. Organomet. Chem.* **1986**, *316*, C13.

[Cp*(DippN=)TaCl(μ -H)]₂ (4). A hexanes solution (50 mL) of **1** (4.80 g, 6.20 mmol) was pressurized (80 psi) with hydrogen at room temperature. After 45 min the color of the solution had changed from deep red to light orange, and a yellow precipitate had formed. The precipitate was collected on a fritted glass filter and was washed twice with hexanes to give pure **4** (2.56 g, 78%). Concentrating and cooling the combined filtrate to -25 °C afforded a second crop of **4** (0.57 g, 17%). Total yield: 3.13 g (96%). ¹H NMR (500 MHz, CD₂Cl₂): δ 7.91 (s, 2 H, Ta-H), 7.09 (m, 4 H, *m*-Ar-H), 6.92 (t, 2 H, *p*-Ar-H, *J* = 8), 3.99, 3.27 (2 \times septet, 2 \times 2 H, ¹Pr-H, *J* = 7), 2.05 (s, 30 H, C₅Me₅), 1.31, 1.21, 1.20, 1.14 (4 \times d, 4 \times 6 H, ¹Pr-Me, *J* = 7). ¹³C{¹H} NMR (100 MHz, CD₂Cl₂): δ 149.1, 148.4, 145.1 (Ar C), 124.9, 122.9, 122.4, (Ar CH), 119.0 (C₅Me₅), 27.3, 27.2, 26.9, 24.8, 24.2, 24.2 (¹Pr), 11.9 (C₅Me₅). IR (KBr, cm⁻¹): 1606 (vs, br, ν _{TaH}). Anal. Calcd for C₄₄H₆₆Cl₂N₂Ta₂ (1055.82): C, 50.05; H, 6.30; N, 2.65. Found: C, 50.45; H, 6.25; N, 2.49.

[Cp*(DippN=)TaCl(μ -D)]₂ (4-d). Selected data: IR (KBr, cm⁻¹): 1151 (vs, br, ν _{TaD}).

{Li(THF)₃}[Cp*(DippN=)Ta(Cl)[Si(SiMe₃)₃H] (5). A THF suspension (20 mL) of **4** (650 mg, 0.62 mmol) and (THF)₃LiSi(SiMe₃)₃ (580 mg, 1.23 mmol) was stirred at room temperature until a clear, yellow solution was obtained (2 h). The solution was filtered and concentrated in vacuo to ca. 10 mL. After the solution was cooled to -30 °C and layered with pentane (20 mL), yellow crystals formed instantly and were allowed to settle. The supernatant liquid was removed by filtration, and the crystals were washed with a few milliliters of cold (-30 °C) pentane and briefly dried in vacuo to isolate **5** (1.09 g, 89%). The bright yellow crystals of **5** can be stored in a closed vial for several weeks with only slight decomposition. Further drying results in loss of coordinated THF and subsequent separation of LiCl, as evidenced by a color change to dark red **6**. Addition of THF reverses the process. ¹H NMR (400 MHz, THF-*d*₆): δ 12.83 (s, 1 H, Ta-H; *J*_{SiH} = 31), 6.73 (t, 2 Ar-H), 6.47 (t, 1 Ar-H), 4.24, 4.18 (2 \times septet, 2 \times 1 H, ¹Pr-H, *J* = 7), 2.01 (s, 15 H, C₅Me₅), 1.14, 1.12, 1.06, 1.00 (4 \times d, 4 \times 3 H, ¹Pr-Me, *J* = 7), 0.13 (s, 27 H, Si(SiMe₃)₃). ⁷Li NMR (194 MHz, 0.06 M in THF-*d*₆): δ -0.33. ¹³C{¹H} NMR (126 MHz, THF-*d*₆): δ 152.7, 145.1, 141.1 (Ar C), 121.2, 121.0, 118.5 (Ar CH), 111.5 (C₅Me₅), 26.0, 25.6, 25.4, 25.0, 24.8, 24.2 (¹Pr), 12.0 (C₅Me₅), 6.1 (SiMe₃). ²⁹Si NMR (99 MHz, THF-*d*₆): δ -0.1 (Si(SiMe₃)₃), -98.4 (Si(SiMe₃)₃), *J*_{SiH} = 31. IR (KBr, cm⁻¹): 1805 (m, br, ν _{TaH}). Anal. Calcd for C₄₃H₈₄ClLiNO₃Si₄Ta (998.83): C, 51.71; H, 8.48; N, 1.40; Cl, 3.55. Found: C, 51.61; H, 8.68; N, 1.65; Cl, 3.33.

{Li(THF)₃}[Cp*(DippN=)Ta(Cl)[Si(SiMe₃)₃D] (5-d). Selected data: IR (KBr, cm⁻¹): 1282 (w, ν _{TaD}).

Cp*(DippN=)Ta[Si(SiMe₃)₃H] (6). A THF (80 mL) solution of complex **4** (2.00 g, 1.89 mmol) and (THF)₃LiSi(SiMe₃)₃ (1.79 g, 3.80 mmol) was stirred at room temperature for 6 h. The THF was removed in vacuo, and the yellow residue was extracted with hexanes (4 \times 20 mL). The combined red extracts were filtered, concentrated to ca. 30 mL, and cooled to -30 °C to afford two crops of dark red crystals of **6** (1.63 g, 58%). ¹H NMR (300 MHz, benzene-*d*₆): δ 21.49 (s, 1 H, Ta-H), 7.21 (t, 2 H, *m*-Ar-H, *J* = 8), 6.95 (t, 1 H, *p*-Ar-H, *J* = 8), 4.30, 3.68 (2 \times septet, 2 \times 1 H, ¹Pr-H, *J* = 7), 1.98 (s, 15 H, C₅Me₅), 1.44, 1.43, 1.27, 1.18 (4 \times d, 4 \times 3 H, ¹Pr-Me, *J* = 7), 0.45 (s, 27 H, Si(SiMe₃)₃). ¹³C{¹H} NMR (100 MHz, benzene-*d*₆): δ 150.7, 146.2, 144.5 (Ar C), 124.7, 123.0, 123.0 (Ar CH), 118.6 (C₅Me₅), 27.9, 27.4, 26.4, 25.8, 25.3, 25.1 (¹Pr), 12.5 (C₅Me₅), 7.0 (Si(SiMe₃)₃). ²⁹Si{¹H} NMR (99 MHz, benzene-*d*₆): δ -1.1 (Si(SiMe₃)₃), -22.9 (Si(SiMe₃)₃). IR (KBr, cm⁻¹): 1785 (w, ν _{TaH}). Anal. Calcd for C₃₁H₆₀NSi₄Ta (740.11): C, 50.31; H, 8.17; N, 1.89. Found: C, 50.52; H, 8.08; N, 1.92.

Cp*(DippN=)Ta[Si(SiMe₃)₃D] (6-d). Selected data: IR (KBr, cm⁻¹): 1276 (w, ν _{TaD}).

{NBu₄}[Cp*(DippN=)Ta(Br)[Si(SiMe₃)₃H] (7). [NBu₄]-Br (ca. 10 mg, 31 μ mol) was added to a THF-*d*₆ solution of **6** (freshly generated from **5** (13 mg, 13 μ mol)) in an NMR tube

fitted with a J. Young Teflon stopper (containing a sealed capillary filled with D₂O), and the mixture was shaken. A color change from red to light yellow occurred within 1 min. The resulting bromide adduct **7** was identified by NMR spectroscopy (quantitative conversion). Selected data: ¹H NMR (500 MHz, THF-*d*₆): δ 12.01 (s, 1 H, Ta-H; *J*_{SiH} = 33), 2.04 (s, 15 H, C₅Me₅), 0.16 (s, 27 H, Si(SiMe₃)₃). ²⁹Si{¹H} NMR (99 MHz, THF-*d*₆): δ -4.8 (Si(SiMe₃)₃), -105.9 (Si(SiMe₃)₃).

{NBu₄}[Cp*(DippN=)Ta(I)[Si(SiMe₃)₃H] (8). An essentially identical procedure to that used to prepare **7** (substituting [NBu₄]I for [NBu₄]Br) yielded **8** as a light yellow solution (quantitative conversion). Selected data: ¹H NMR (500 MHz, THF-*d*₆): δ 10.71 (s, 1 H, Ta-H; *J*_{SiH} = 36), 2.09 (s, 15 H, C₅Me₅), 0.18 (s, 27 H, Si(SiMe₃)₃). ²⁹Si{¹H} NMR (99 MHz, THF-*d*₆): δ -3.8 (Si(SiMe₃)₃), -112.4 (Si(SiMe₃)₃).

Cp*(DippN=)Ta[η -C(N-2,6-Me₂C₆H₃)Si(SiMe₃)₃H] (9). A toluene solution (15 mL) of complex **6** (450 mg, 0.608 mmol) and xylyl isocyanide (94 mg, 0.72 mmol) was stirred at room temperature for 6 h. The initial red solution gradually turned brown-orange. The solvent was removed in vacuo, and the residue was extracted with pentane (20 mL). The orange solution was filtered and cooled to -25 °C to afford light orange crystals of **9** (257 mg, 49%). ¹H NMR (300 MHz, benzene-*d*₆): δ 10.14 (s, 1 H, Ta-H), 7.20, 7.10 (2 \times m, 2 \times 1 Ar-H), 6.97-6.82 (m, 4 Ar-H), 4.44, 3.75 (2 \times septet, 2 \times 1 H, ¹Pr-H, *J* = 7), 2.28 (s, 3 H, Xylyl-Me), 1.91 (s, 15 H, C₅Me₅), 1.78 (s, 3 H, Xylyl-Me), 1.53, 1.49, 1.36, 1.15 (4 \times d, 4 \times 3 H, ¹Pr-Me, *J* = 7), 0.20 (s, 27 H, Si(SiMe₃)₃). ¹³C{¹H} NMR (100 MHz, benzene-*d*₆): δ 280.2 (CNXylyl), 152.8, 149.4, 142.1, 141.6, 131.0, 129.8, 129.5, 129.1, 127.0, 123.0, 122.5, 121.4 (Ar C, CH), 113.5 (C₅Me₅), 27.1, 26.7, 26.1, 25.9 (br), 21.3, 19.3 (¹Pr, Xylyl-Me), 12.0 (C₅Me₅), 2.9 (Si(SiMe₃)₃). ²⁹Si{¹H} NMR (60 MHz, benzene-*d*₆): δ -10.7 (Si(SiMe₃)₃), -80.6 (Si(SiMe₃)₃). IR (KBr, cm⁻¹): 1782 (s, ν _{TaH}), 1587 (w, ν _{C=N}), 1531 (m, ν _{C=N}). Anal. Calcd for C₄₀H₆₉N₂Si₄Ta (871.29): C, 55.14; H, 7.98; N, 3.22. Found: C, 55.08; H, 8.31; N, 3.15.

Cp*(DippN=)Ta[C=N(Me)Si(SiMe₃)₃H] (10). A benzene-*d*₆ solution (~0.7 mL) of complex **6** (34.0 mg, 0.046 mmol) was transferred to an NMR tube capped with a septum, and acetonitrile (1.9 mg, 0.046 mmol) was added to the NMR tube via syringe. Upon addition, the reaction mixture changed from dark red to bright yellow. The conversion to **10** was determined to be >95% (by integration of the Cp* resonances in the ¹H NMR spectrum of the reaction mixture). After 18 h at room temperature, most of **10** had decomposed to unidentified species. ¹H NMR (500 MHz, benzene-*d*₆): δ 12.60 (s, 1 H, Ta-H), 7.17-6.96 (m, 3 H, Ar-H), 4.23, 3.60 (2 \times septet, 2 \times 1 H, ¹Pr-H, *J* = 7), 1.92 (s, 15 H, C₅Me₅), 1.43, 1.30, 1.30, 1.12 (4 \times d, 4 \times 3 H, ¹Pr-Me, *J* = 7), 1.39 (s, 3 H, N=CMe), 0.44 (s, 27 H, Si(SiMe₃)₃).

Cp*(DippN=)Ta(OⁱPr)[Si(SiMe₃)₃] (11). An essentially identical procedure to that used to prepare **10** (substituting acetone for acetonitrile) yielded a bright yellow solution of **11** in >95% conversion. No change was observed in the spectrum after 2 days at room temperature. ¹H NMR (300 MHz, benzene-*d*₆): δ 7.15 (m, 2 Ar-H), 6.91 (m, 1 Ar-H), 4.88 (septet, 1 H, OCHMe₂, *J* = 6), 3.84, 3.52 (2 \times septet, 2 \times 1 H, ¹Pr-H, *J* = 7), 1.97 (s, 15 H, C₅Me₅), 1.39, 1.35, 1.29, 1.27 (4 \times d, 4 \times 3 H, ¹Pr-Me, *J* = 7), 1.25, 1.18 (2 \times d, 2 \times 3 H, OCHMe₂, *J* = 6), 0.47 (s, 27 H, Si(SiMe₃)₃). ¹³C{¹H} NMR (126 MHz, benzene-*d*₆): δ 151.3, 145.3, 144.2 (Ar C), 124.1, 123.7, 123.0 (Ar CH), 117.9 (C₅Me₅), 78.3 (OCHMe₂), 28.4, 27.7, 27.3, 27.0, 25.7, 25.4, 25.3, 22.9 (¹Pr), 13.0 (C₅Me₅), 7.0 (SiMe₃).

Cp*(DippN=)Ta[CH₂CH₂CH₂CH₂] (12). Exposure of a stirred suspension of **6** in pentane (10 mL) to ethylene (1 atm) for a few seconds gave a clear yellow solution. After stirring for an additional 5 min, the solution was filtered, concentrated in vacuo to a few milliliters, and cooled to -30 °C to afford three crops of yellow crystals, which were isolated, washed with a little cold pentane, and dried in vacuo to give pure **12**

(82 mg, 75%). ¹H NMR (400 MHz, benzene-*d*₆): δ 7.25 (d, 2 Ar-H), 6.99 (t, 1 Ar-H), 3.72 (septet, 2 H, ⁱPr-H, *J* = 7), 2.47, 2.23 (2 × m, 2 × 2 H, α-CH₂), 1.73 (s, 15 H, C₅Me₅), 1.68 (m, 2 H, β-CH₂), 1.38 (d, 12 H, ⁱPr-Me, *J* = 7), 0.96 (m, 2 H, β-CH₂). ¹³C{¹H} NMR (101 MHz, benzene-*d*₆): δ 152.1, 144.4 (Ar C), 122.6 (Ar CH), 116.3 (C₅Me₅), 53.9 (α-CH₂), 28.6 (CHMe₂), 24.8 (CHMe₂), 16.6 (β-CH₂), 11.0 (C₅Me₅). MS: *m/z* 547 (24, [M]⁺), 519 (28), 489 (100), 487 (88), 445 (16), 244 (10). Anal. Calcd for C₂₆H₄₀N₂Ta (547.56): C, 57.03; H, 7.36; N, 2.56. Found: C, 57.00; H, 7.11; N, 2.61.

Cp*(DippN=)Ta[CPhCPhCPhCPh] (13). A benzene-*d*₆ (~0.7 mL) solution of complex **6** (20.0 mg, 0.0270 mmol) and diphenylacetylene (9.6 mg, 0.054 mmol) was transferred to an NMR tube fitted with a J. Young Teflon stopper. After 24 h (room temperature), the conversion to **13** was determined to be 52% (by integration of the Cp* resonances in the ¹H NMR spectrum of the reaction mixture). ¹H NMR (500 MHz, benzene-*d*₆): δ 7.37–6.63 (m, 23 Ar-H), 5.04 (septet, 2 H, ⁱPr-H, *J* = 6), 1.86 (s, 15 H, C₅Me₅), 1.52 (d, 12 H, ⁱPr-Me, *J* = 6).

[Cp*(DippN=)TaH(μ-H)]₂ (14). A hexanes (20 mL) solution of **6** (0.51 g, 0.69 mmol) was pressurized (60 psi) with hydrogen at room temperature. After 15 min, the color of the solution had changed from red to yellow, and a fine yellow precipitate had settled. The precipitate was collected on a fritted glass filter and was washed with hexanes to yield pure **14** (0.19 g, 56%). ¹H NMR (400 MHz, benzene-*d*₆): δ 15.54 (t, 2 H, Ta-H, *J* = 8), 7.17 (m, 4 H, *m*-Ar-H), 6.96 (t, 2 H, *p*-Ar-H, *J* = 8), 6.48 (t, 2 H, Ta-(μ-H), *J* = 8), 4.67, 3.83 (2 × septet, 2 × 2 H, ⁱPr-H, *J* = 7), 2.05 (s, 30 H, C₅Me₅), 1.43, 1.37, 1.35, 1.32 (4 × d, 4 × 6 H, ⁱPr-Me, *J* = 7). ¹³C{¹H} NMR (100 MHz, benzene-*d*₆): δ 151.2, 144.9, 144.1 (Ar C), 123.9, 122.8, 122.7, (Ar CH), 115.4 (C₅Me₅), 27.5, 27.3, 25.8, 25.4, 24.2, 24.0 (ⁱPr), 12.7 (C₅Me₅). IR (KBr, cm⁻¹): 1771 (m, ν_{TaH}), 1529 (s, br, ν_{Ta-(μ-H)}). Anal. Calcd for C₄₄H₆₈N₂Ta₂ (986.93): C, 53.55; H, 6.94; N, 2.84. Found: C, 53.54; H, 6.98; N, 2.90.

Cp*(DippN=)Ta[CH₂Si(SiMe₃)₂SiMe₂H]H (15). A solution of **6** (freshly generated from **5** (88 mg, 0.088 mmol)) in benzene (5 mL) was stirred at room temperature for 48 h. The resulting clear yellow solution was filtered, and the solvent and volatile byproducts were removed in vacuo to give an orange oil, which consisted mainly of a 2:1 mixture of **15** (ca. 60%) and HSi(SiMe₃)₃, along with minor impurities (one of which is **18**, see below). Numerous attempts to separate **15** by crystallization from a variety of solvents failed. Decomposition rate: *t*_{1/2} = 8.5 h (by NMR). ¹H NMR (500 MHz, benzene-*d*₆): δ 9.58 (dd, 1 H, Ta-H, *J* = 9, 4), 7.07 (d, 2 H, *m*-Ar-H, *J* = 8), 6.88 (t, 1 H, *p*-Ar-H, *J* = 8), 4.10 (septet, 2 H, ⁱPr-H, *J* = 7), 2.57 (dddq, 1 H, SiH, *J* = 9, 4, 1), 1.96 (s, 15 H, C₅Me₅), 1.35, 1.29 (2 × d, 2 × 6 H, ⁱPr-Me, *J* = 7), 0.70 (ddd, 1 H, TaCH₂Si, *J* = 13, 4; *J*_{CH} = 129), 0.43 (d, 3 H, SiMe, *J* = 4), 0.24, 0.22 (2 × s, 2 × 9 H, Si(SiMe₃)₂), -0.09 (s, 3 H, SiMe), -0.90 (dd, 1 H, TaCH₂Si, *J* = 13, 1; *J*_{CH} = 129). ¹³C{¹H} NMR (126 MHz, benzene-*d*₆): δ 151.2, 144.1 (Ar C), 123.4 (*p*-Ar CH), 122.4 (*m*-Ar CH), 113.2 (C₅Me₅), 27.6 (ⁱPr CH), 24.9, 24.4 (ⁱPr Me), 11.9 (C₅Me₅), 10.8 (TaCH₂Si), 0.7, 0.6 (SiMe₃), -1.8, -11.8 (SiMe₂H). ²⁹Si NMR (99 MHz, benzene-*d*₆): δ -10.5, -11.1 (Si(SiMe₃)₂), -68.9 (HSiMe₂, ¹*J*_{SiH} = 87), -88.3 (Si(SiMe₃)₂). Temperature-dependence of ¹*J*_{SiH}: 78 Hz at -70 °C; 101 Hz at 80 °C. MS: *m/z* 739 (5, [M]⁺), 737 (56, [M - H₂]⁺), 693 (19), 664 (84), 622 (33), 562 (20), 546 (15), 489 (16), 248 (41), 233 (31), 174 (97), 160 (50), 73 (100). IR (neat decomp mixture, film) on KBr, cm⁻¹): 2052 (m, ν_{SiH} of HSi(SiMe₃)₃), 1726 (m, ν_{SiH}).

Me₂HSi-Si(SiMe₃)₂Me.⁴⁶ This compound was obtained by hydrolysis of **15** with H₂O. ¹H NMR (500 MHz, benzene-*d*₆): δ 4.20 (septet, 1 H, SiH, *J* = 4.5, *J*_{SiH} = 175), 0.23 (d, 6 H, HSiMe₂, *J* = 4), 0.19 (s, 18 H, SiMe(SiMe₃)₂), 0.12 (s, 3 H, SiMe(SiMe₃)₂). ¹³C{¹H} NMR (126 MHz, benzene-*d*₆): δ 0.6 (SiMe₃), -3.7 (br, HSiMe₂), -12.9 (SiMe(SiMe₃)₂). ²⁹Si{¹H} NMR (99 MHz, benzene-*d*₆): δ -11.9 (SiMe(SiMe₃)₂), -34.2

(br, SiH), -87.7 (SiMe(SiMe₃)₂). GCMS: *m/z* 248 (3, [M]⁺), 233 (9, [M - Me]⁺), 189 (5), 174 (100, [M - HSiMe₃]⁺), 159 (51), 145 (11), 131 (22), 129 (23), 115 (21), 101 (12), 85 (5), 73 (86), 59 (15), 45 (16).

Cp*(DippN=)Ta[η²-C(N-2,6-Me₂C₆H₃)CH₂Si(SiMe₃)₂-SiMe₂H]H (16). Xylyl isocyanide (9.1 mg, 0.069 mmol) was added to a solution of **15** and HSi(SiMe₃)₃ (freshly prepared from **6** (70 mg, 0.070 mmol) in benzene-*d*₆ (2 mL), 36 h reaction time). A dark brown-orange solution formed within 15 min, and the reaction mixture was stirred for an additional 1 h. The solvents were removed in vacuo to yield a dark brown oil, which resisted all crystallization attempts (the conversion of **15** to **16** was quantitative by ¹H NMR). ¹H NMR (500 MHz, benzene-*d*₆): δ 10.26 (d, 1 H, Ta-H, *J* = 1), 7.11 (d, 2 H, *m*-Ar-H, *J* = 8), 6.89–6.81 (m, 4 Ar-H), 3.83 (ddq, 1 H, Si-H, *J* = 10, 5, 2), 3.75 (septet, 2 H, ⁱPr-H, *J* = 7), 1.95 (br s, 6 H, Xylyl-Me), 1.84 (s, 15 H, C₅Me₅), 1.38 (m, 12 H, ⁱPr-Me), 0.64 (ddd, 1 H, TaCH₂Si, *J* = 13, 9, 1), 0.32 (s, 9 H, SiMe₃), 0.29 (s, 3 H, SiMe), 0.22 (s, 9 H, SiMe₃), 0.05 (d, 3 H, SiMe, *J* = 5), -0.07 (dd, 1 H, TaCH₂Si, *J* = 13, 2). ¹³C{¹H} NMR (126 MHz, benzene-*d*₆): δ 242.0 (CNXylyl), 151.6, 146.9 (Ar C), 129.3 (br, *m*-Ar CH), 126.8 (*p*-Ar CH), 122.6 (br, *m*-Ar CH), 122.1 (*p*-Ar CH), 114.3 (C₅Me₅), 27.2 (ⁱPr CH), 26.5, 24.7 (br, ⁱPr Me), 19.3 (br, Xylyl-Me), 18.9 (TaCH₂Si), 11.6 (C₅Me₅), 1.1, 1.0 (SiMe₃), -2.0, -11.8 (SiMe). ²⁹Si NMR (99 MHz, benzene-*d*₆): δ -11.6, -11.7 (SiMe(SiMe₃)₂), -27.2 (HSiMe₂, ¹*J*_{SiH} = 174), -84.3 (Si(SiMe₃)₂). MS: *m/z* 870 (6, [M]⁺), 855 (2), 681 (100), 248 (8), 233 (6), 174 (12), 162 (14), 73 (18).

Cp*(DippN=)Ta(OCHPh₂)[CH₂Si(SiMe₃)₂SiMe₂H] (17). A hexanes (15 mL) solution of benzophenone (36 mg, 0.20 mmol) was added to a solution of **15** and HSi(SiMe₃)₃ (freshly prepared from **6** (196 mg, 0.200 mmol) in hexanes (15 mL), 72 h reaction time). A color change from orange to bright yellow occurred instantly. After stirring the reaction mixture at room temperature for 1 h, the solvent was removed in vacuo to yield an orange oil, which resisted all crystallization attempts (the conversion of **15** to **17** was quantitative by ¹H NMR). ¹H NMR (500 MHz, benzene-*d*₆): δ 7.47 (m, 2 *o*-Ph-H), 7.43 (m, 2 *o*-Ph-H), 7.19–6.99 (m, 8 Ar-H), 6.90 (m, 1 H, *p*-Ar-H), 6.74 (s, 1 H, OCHPh₂), 3.99 (dq, 1 H, Si-H, *J* = 10, 4), 3.71 (septet, 2 H, ⁱPr-H, *J* = 7), 1.82 (s, 15 H, C₅Me₅), 1.30 (t, 12 H, ⁱPr-Me, *J* = 7), 0.90 (dd, 1 H, TaCH₂Si, *J* = 13, 10), 0.47 (d, 1 H, TaCH₂-Si, *J* = 13), 0.28 (s, 9 H, SiMe₃), 0.24 (s, 3 H, SiMe), 0.22 (s, 9 H, SiMe₃), 0.19 (d, 3 H, SiMe, *J* = 4). ¹³C{¹H} NMR (126 MHz, benzene-*d*₆): δ 151.0, 145.9, 145.8, 144.1 (Ar C), 128.9–122.9 (Ar CH), 117.3 (C₅Me₅), 89.0 (OCHPh₂), 30.6 (TaCH₂), 27.9, 26.5, 26.0, 24.8 (ⁱPr), 11.4 (C₅Me₅), 1.0 (SiMe₃), -2.3 (SiMe), -12.2 (SiMe). ²⁹Si NMR (99 MHz, benzene-*d*₆): δ -11.6, -11.7 (SiMe(SiMe₃)₂), -27.4 (HSiMe₂, ¹*J*_{SiH} = 183), -83.6 (Si(SiMe₃)₂). MS: *m/z* 921 (1, [M]⁺), 906 (2), 746 (5), 732 (62), 689 (10), 636 (7), 579 (9), 565 (47), 522 (6), 248 (7), 233 (4), 182 (11), 174 (12), 167 (100, [CHPh₂]⁺), 105 (14), 73 (14).

{Cp*(DippN=)Ta[CH₂Si(SiMe₃)₂SiMe₂H]}(μ-H)₂{TaCp*(=NDipp)H} (18). Complex **18** was isolated as orange crystals from cold pentane solutions of the reaction mixture resulting from decomposition of **6** (ca. 5% yield). ¹H NMR (500 MHz, benzene-*d*₆): δ 14.93 (dd, 1 H, Ta-H, *J* = 9, 6), 7.17 (dd, 1 *m*-Ar-H, *J* = 8, 2), 7.12 (m, 3 *m*-Ar-H), 6.99 (m, 1 H, Ta-(μ-H)), 6.96–6.90 (m, 2 *p*-Ar-H), 6.63 (dd, 1 H, Ta-(μ-H), *J* = 6, 4), 4.69 (m, 1 H, Si-H), 4.39, 4.15, 3.90, 3.69 (4 × septet, 4 × 1 H, ⁱPr-H, *J* = 7), 2.05, 1.98 (2 × s, 2 × 15 H, C₅Me₅), 1.482, 1.478, 1.45, 1.42, 1.37, 1.36, 1.32, 1.29 (8 × d, 8 × 3 H, ⁱPr-Me, *J* = 7), 0.96 (dd, 1 H, TaCH₂Si, *J* = 12, 9), 0.68 (d, 3 H, SiMe, *J* = 4), 0.44 (s, 3 H, SiMe), 0.41, 0.38 (2 × s, 2 × 9 H, SiMe(SiMe₃)₂), -0.57 (dd, 1 H, TaCH₂Si, *J* = 12, 3). ¹³C{¹H} NMR (126 MHz, benzene-*d*₆): δ 151.8, 147.8, 144.6 (Ar C), 124.4, 123.9, 123.7, 123.0, 122.9, 122.7 (Ar CH), 117.3, 114.6 (C₅Me₅), 34.5 (TaCH₂-Si), 28.2, 27.5, 27.2, 26.3 (ⁱPr CH), 26.7, 26.1, 25.9, 25.8, 25.1, 24.1, 23.4 (ⁱPr Me), 12.8, 12.4 (C₅Me₅), 1.3, 0.9 (SiMe₃), 0.0, -11.2 (SiMe₂H). ²⁹Si{¹H} NMR (99 MHz, benzene-*d*₆): δ -11.2, -11.7 (SiMe(SiMe₃)₂), -29.4 (HSiMe₂), -84.1 (SiMe(SiMe₃)₂).

IR (KBr, cm^{-1}): 2086 (m, ν_{SiH}), 1794 (w, ν_{TaH}), 1619 (m, br, $\nu_{\text{Ta-(u-H)}}$), 1508 (m, br, $\nu_{\text{Ta-(u-H)}}$). Anal. Calcd for $\text{C}_{53}\text{H}_{94}\text{N}_2\text{Si}_4\text{Ta}_2$ (1233.58): C, 51.60; H, 7.68; N, 2.27. Found: C, 51.34; H, 7.81; N, 2.10.

{Li(THF)₃}{Cp*(DippN=)TaCl(SiPh₃)H} (19). A THF (15 mL) suspension of complex **4** (200 mg, 0.189 mmol) and (THF)₃LiSiPh₃ (170 mg, 0.352 mmol) was stirred at room temperature until a clear orange solution was obtained (1 h). The solution was concentrated in vacuo to ca. 7 mL and then layered with pentane (30 mL) and cooled to -78°C . After 4 h, the dark yellow oil that formed was separated from the supernatant liquid, dried in vacuo, and then extracted into pentane (30 mL). The extracts were filtered, concentrated to half volume (ca. 15 mL), and cooled to -78°C for 24 h. The resulting precipitate was isolated by filtration and dried in vacuo to give **19** (225 mg, 66%) as a bright yellow powder. Complex **19** can be stored at -40°C for a few days. ¹H NMR (500 MHz, THF-*d*₆): δ 11.97 (s, 1 H, Ta-H, $J_{\text{SiH}} = 34$), 7.57 (m, 6 H, *o*-Ph-H), 6.94 (m, 6 H, *m*-Ph-H), 6.88 (m, 3 H, *p*-Ph-H), 6.80–6.64 (br m, 2 H, *m*-Ar-H), 6.49 (t, 1 H, *p*-Ar-H), 4.11 (br s, 2 H, ¹Pr-H), 1.80 (s, 15 H, C₅Me₅), 1.19, 1.08, 1.02, 0.38 (4 \times br s, 4 \times 3 H, ¹Pr-Me). ¹³C{¹H} NMR (126 MHz, THF-*d*₆): δ 154.2 (Ar C), 153.3 (Ph C), 139.1 (br, *o*-Ph CH), 127.2 (br, *m*-Ph CH), 126.4 (br, *p*-Ph CH), 122.3 (br, *m*-Ar CH), 120.2 (*p*-Ar CH), 111.9 (C₅Me₅), 28.4 (br, ¹Pr CH), 27.2, 25.3, 24.7 (br, ¹Pr Me), 12.8 (C₅Me₅). ²⁹Si{¹H} NMR (99 MHz, THF-*d*₆): δ 47.6. ¹H NMR (400 MHz, benzene-*d*₆): δ 13.11 (s, 1 H, Ta-H, $J_{\text{SiH}} = 32$), 8.02 (m, 6 H, *o*-Ph-H), 7.18 (m, 6 H, *m*-Ph-H), 7.04 (m, 3 H, *p*-Ph-H), 7.01 (br m, 2 H, *m*-Ar-H), 6.85 (t, 1 H, *p*-Ar-H), 4.36, 4.00 (2 \times br m, 2 \times 1 H, ¹Pr-H), 3.08 (m, 12 H, THF), 2.02 (s, 15 H, C₅Me₅), 1.39, 1.30 (2 \times br d, 2 \times 3 H, ¹Pr-Me, $J = 7$), 1.18 (m, 12 H, THF), 1.14, 1.06 (2 \times br d, 2 \times 3 H, ¹Pr-Me, $J = 7$). ⁷Li NMR (194 MHz, 0.06 M in THF): δ -0.264. ¹³C{¹H} NMR (101 MHz, benzene-*d*₆): δ 152.5 (Ar C), 150.0 (Ph C), 138.1 (*o*-Ph CH), 127.8 (*m*-Ph CH), 127.4 (*p*-Ph CH), 122.4 (br, *m*-Ar CH), 122.4 (*p*-Ar CH), 112.5 (C₅Me₅), 68.1 (THF), 27.5 (br, ¹Pr CH), 26.3, 25.9 (br, ¹Pr Me), 25.7 (THF), 25.3, 23.4 (br, ¹Pr Me), 12.0 (C₅Me₅). ²⁹Si{¹H} NMR (99 MHz, benzene-*d*₆): δ 47.2 (br). IR (KBr, cm^{-1}): 1820 (m, br, $\nu_{\text{Ta-H}}$). Anal. Calcd for $\text{C}_{52}\text{H}_{72}\text{ClLiNO}_3\text{SiTa}$ (1010.58): C, 61.80; H, 7.18; N, 1.39. Found: C, 61.79; H, 6.85; N, 1.53.

Cp*(DippN=)Ta[η^2 -CH₂(2-SiH₂Mes-3,5-Me₂C₆H₂)]H (20). Complex **4** (500 mg, 0.474 mmol) and (THF)₂LiSiHMe₂ (396 mg, 0.946 mmol) were dissolved in cold (-80°C) Et₂O (150 mL). The stirred reaction mixture was then allowed to warm to room temperature, and stirring was continued for a total reaction time of 12 h. The solvent was removed in vacuo from the clear orange solution, and the resulting residue was extracted with hexanes (50 mL). The extracts were filtered, concentrated, and cooled to -25°C to afford bright yellow crystals of **20** (50 mg, 7%). Removal of the solvent from the supernatant in vacuo gave a yellow foam which consisted of a 4:1 mixture of **20** and H₂SiMe₂. ¹H NMR (300 MHz, benzene-*d*₆): δ 8.62 (s, 1 H, Ta-H), 7.17 (d, 2 H, *m*-Ar-H, $J = 8$), 6.97 (t, 1 H, *p*-Ar-H, $J = 8$), 6.60 (s, 2 H, Mes-H), 6.34, 5.51 (2 \times s, 2 \times 1 Mes-H), 5.14 (d, 1 H, Si-H, $J = 4$, $^1J_{\text{SiH}} = 205$), 5.03 (d, 1 H, Si-H, $J = 4$, $^1J_{\text{SiH}} = 213$), 4.24 (br s, 2 H, ¹Pr-H), 3.60 (d, 1 H, Ta-CH₂, $J = 7$), 2.30 (s, 3 H, Mes-Me), 2.28 (s, 6 H, Mes-Me), 2.07, 2.02 (2 \times s, 2 \times 3 H, Mes-Me), 1.91 (s, 15 H, C₅Me₅), 1.90 (hidden d, 1 H, Ta-CH₂), 1.44 (d, 6 H, ¹Pr-Me, $J = 7$), 1.41 (br s, 6 H, ¹Pr-Me). ¹³C{¹H} NMR (100 MHz, benzene-*d*₆): δ 152.1, 149.2, 145.2, 144.1, 141.5, 139.3, 130.2, 129.7, 129.3, 125.3, 122.9 (br) (Ar C, CH), 113.1 (C₅Me₅), 53.1 (Ta-CH₂), 32.3, 27.4, 26.0, 25.4 (br), 24.0, 23.9, 22.2, 21.5 (¹Pr, Me), 12.3 (C₅Me₅). ²⁹Si{¹H} NMR (99 MHz, benzene-*d*₆): δ -56.2. IR (KBr, cm^{-1}): 2194 (m, ν_{SiH}), 2183 (m, ν_{SiH}), 1778 (m, ν_{TaH}). Anal. Calcd for $\text{C}_{40}\text{H}_{56}\text{NSiTa}$ (759.93): C, 63.22; H, 7.43; N, 1.84. Found: C, 63.59; H, 7.88; N, 1.91.

{Li(THF)_n}{Cp*(DippN=)TaCl[SiH(2,4,6-Me₃C₆H₂)]H} (21). Complex **4** (24.5 mg, 0.0232 mmol) and (THF)₂LiSiHMe₂ (19.4 mg, 0.0463 mmol) were dissolved in

cold (-30°C) THF-*d*₆ in an NMR tube fitted with a J. Young Teflon stopper. The reaction mixture instantly became deep purple in color. The NMR tube was transferred to the precooled NMR probe, and the reaction progress was followed by ¹H NMR spectroscopy while the probe was slowly warmed to room temperature in order to observe the formation of **21**. After ca. 5 min, **21** was completely converted to **20** and several unidentified decomposition products. ¹H NMR (500 MHz, THF-*d*₆): δ 12.26 (s, 1 H, Ta-H; $J_{\text{SiH}} = 33$), 6.77 (d, 2 Ar-H), 6.61 (t, 1 Ar-H), 6.48, 6.42 (2 \times s, 2 \times 2 Ar-H), 5.38 (s, 1 H, Si-H, $^1J_{\text{SiH}} = 146$), 4.24 (septet, 2 H, ¹Pr-H, $J = 7$), 2.40, 2.37, 2.30 (3 \times s, 3 \times 6 H, Mes-Me), 1.88 (s, 15 H, C₅Me₅), 1.06 (d, 12 H, ¹Pr-Me, $J = 7$).

Cp*(DippN=)TaMe₂ (22). A solution of MeMgBr in diethyl ether (0.25 mL, 1.4 M, 0.35 mmol) was added dropwise via syringe to a stirred suspension of **4** (186 mg, 0.176 mmol) in diethyl ether (30 mL). After 30 min, a clear yellow solution had formed. The solvent was removed in vacuo, and the residue was extracted with hexanes (2 \times 10 mL). The combined extracts were filtered, concentrated, and cooled to -25°C to afford **22** (88 mg, 48%) as a yellow powder. ¹H NMR (300 MHz, benzene-*d*₆): δ 7.22 (d, 2 H, *m*-Ar-H, $J = 8$), 6.96 (t, 1 H, *p*-Ar-H, $J = 8$), 3.69 (septet, 2 H, ¹Pr-H, $J = 7$), 1.71 (s, 15 H, C₅Me₅), 1.36 (d, 12 H, ¹Pr-Me, $J = 7$), 0.30 (s, 6 H, Ta-Me).

Cp*(DippN=)Ta[Si(SiMe₃)₃]Me (23). A solution of MeMgBr in diethyl ether (0.62 mL, 3.0 M, 1.8 mmol) was added dropwise via syringe to a stirred solution of **1** (1.30 g, 1.68 mmol) in diethyl ether (30 mL) at -50°C . The reaction mixture was stirred at -50°C for 30 min and then slowly warmed to room temperature. After 2 days, the solvent was removed in vacuo, and the residue was extracted with pentane (2 \times 15 mL). The combined extracts were filtered, concentrated, and cooled to -30°C to yield large red-orange crystals of **23** (702 mg, 55%). ¹H NMR (500 MHz, benzene-*d*₆): δ 7.20, 7.17 (2 \times dd, 2 \times 1 H, *m*-Ar-H, $J = 8$, 2), 6.94 (t, 1 H, *p*-Ar-H, $J = 8$), 3.91 (septet, 1 H, ¹Pr-H, $J = 7$), 3.67 (septet, 1 H, ¹Pr-H, $J = 7$), 1.87 (s, 15 H, C₅Me₅), 1.46, 1.30 (2 \times d, 2 \times 3 H, ¹Pr-Me, $J = 7$), 1.42, 1.17 (2 \times d, 2 \times 3 H, ¹Pr-Me, $J = 7$), 0.43 (s, 27 H, Si(SiMe₃)₃), 0.28 (s, 3 H, Ta-Me). ¹³C{¹H} NMR (126 MHz, benzene-*d*₆): δ 151.2, 147.5, 145.2 (Ar C), 124.6, 123.6, 123.1 (Ar CH), 118.0 (C₅Me₅), 72.7 (Ta-Me), 27.6, 27.5, 27.2, 26.2, 25.3, 24.7 (¹Pr), 12.3 (C₅Me₅), 6.1 (Si(SiMe₃)₃). ²⁹Si{¹H} NMR (99 MHz, benzene-*d*₆): δ -3.6 (Si(SiMe₃)₃), -54.1 (Si(SiMe₃)₃). MS: m/z 753 (18, [M]⁺), 738 (10, [M - Me]⁺), 606 (11), 562 (84), 489 (100). Anal. Calcd for $\text{C}_{32}\text{H}_{62}\text{NSi}_4\text{Ta}$ (754.14): C, 50.97; H, 8.29; N, 1.86. Found: C, 51.22; H, 8.60; N, 1.92.

Cp*(DippN=)Ta[η^2 -COSi(SiMe₃)₂]Me (24). A benzene-*d*₆ solution (~0.7 mL) of compound **23** (13 mg, 0.017 mmol) was transferred to an NMR tube fitted with a J. Young Teflon stopper. The NMR tube was then sealed under CO (1 atm) and was shaken. Within 1 min, the color of the solution had changed from red-orange to red. After 1 h, the solvent and volatile byproducts were removed in vacuo and the resulting residue was extracted with pentane. The extracts were filtered and cooled to -30°C to afford two crops of dark red needles of **24** (11.6 mg, 86%). ¹H NMR (500 MHz, benzene-*d*₆): δ 7.10 (d, 2 H, *m*-Ar-H, $J = 8$), 6.88 (t, 1 H, *p*-Ar-H, $J = 8$), 3.63 (br s, 2 H, ¹Pr-H), 1.82 (s, 15 H, C₅Me₅), 1.53, 1.36, 1.32, 1.13 (4 \times br s, 4 \times 3 H, ¹Pr-Me), 0.66 (s, 3 H, Ta-Me), 0.27 (s, 27 H, Si(SiMe₃)₃). ¹H NMR (500 MHz, toluene-*d*₈, -40°C): δ 7.09 (d, 2 H, *m*-Ar-H, $J = 8$), 6.88 (t, 1 H, *p*-Ar-H, $J = 8$), 3.64, 3.57 (2 \times septet, 2 \times 1 H, ¹Pr-H, $J = 7$), 1.81 (s, 15 H, C₅Me₅), 1.58, 1.41, 1.36, 1.13 (4 \times d, 4 \times 3 H, ¹Pr-Me, $J = 7$), 0.68 (s, 3 H, Ta-Me), 0.29 (s, 27 H, Si(SiMe₃)₃). ¹³C{¹H} NMR (126 MHz, benzene-*d*₆): δ 408.6 (COSi), 152.0 (Ar C), 122.6 (Ar CH), 114.1 (C₅Me₅), 27.9, 26.0, 23.7 (br, ¹Pr), 27.5, 27.2, 26.2, 25.3, 24.7 (¹Pr), 19.0 (Ta-Me), 10.8 (C₅Me₅), 1.9 (Si(SiMe₃)₃). ²⁹Si{¹H} NMR (99 MHz, benzene-*d*₆): δ -10.0 (Si(SiMe₃)₃), -69.0 (Si(SiMe₃)₃). IR (KBr, cm^{-1}): 1421 (w, ν_{CO} , from difference spectrum), MS: m/z 809 (18, [M + CO]⁺), 781 (26, [M]⁺), 766 (8, [M - Me]⁺), 753 (13, [M - CO]⁺), 738 (12, [M - CO - Me]⁺),

Table 5. Crystallographic Data for Compounds 5·(THF)₂, 6, 20, and 26

	5·(THF) ₂	6	20	26
empirical formula	C ₅₁ H ₁₀₀ ClLiNO ₅ Si ₄ Ta	C ₃₁ H ₆₀ NSi ₄ Ta	C ₄₀ H ₅₆ NSi ₄ Ta	C ₂₇ H ₄₄ NTa
fw	1143.04	740.11	759.91	563.60
cryst color, habit	yellow, polyhedral	red, bladelike	clear, tablet	yellow, block
cryst size (mm)	0.20 × 0.20 × 0.15	0.30 × 0.10 × 0.04	0.15 × 0.08 × 0.20	0.30 × 0.35 × 0.25
cryst syst	monoclinic	triclinic	monoclinic	monoclinic
space group	<i>Pn</i> (No. 7)	<i>P</i> $\bar{1}$ (No. 2)	<i>P</i> ₂ / <i>n</i> (No. 14)	<i>P</i> ₂ / <i>n</i> (No. 14)
<i>a</i> (Å)	12.9227(1)	9.7681(5)	17.0897(2)	9.2331(2)
<i>b</i> (Å)	13.3346(2)	12.0615(6)	11.8106(1)	17.3250(4)
<i>c</i> (Å)	18.4519(1)	16.9644(9)	18.9848(2)	16.8832(3)
α (deg)	90	97.956(1)	90	90
β (deg)	105.745(1)	102.623(1)	107.403(1)	99.062(1)
γ (deg)	90	104.770(1)	90	90
<i>V</i> (Å ³)	3060.31(5)	1845.6(2)	3656.48(7)	2666.99(9)
orientation reflns: number,	7706, 3.0–46.0	7800, 3.0–45.0	7165, 3.0–45.0	7759, 3.0–45.0
2θ range (deg)				
<i>Z</i>	2	2	4	4
<i>D</i> _{calc} (g/cm ³)	1.240	1.332	1.380	1.404
<i>F</i> ₀₀₀	1204.00	764.00	1552.00	1140.00
μ (Mo K α) (cm ⁻¹)	19.55	31.22	30.61	41.27
diffractometer radiation			SMART Mo K α (λ = 0.71069 Å) graphite-monochromated	
temperature (K)	173(1)	115(1)	134(1)	183(1)
scan type	ω (0.3° per frame)	ω (0.3° per frame)	ω (0.3° per frame)	ω (0.3° per frame)
scan rate	10.0 s per frame	10.0 s per frame	10.0 s per frame	10.0 s per frame
data collected, $2\theta_{\max}$ (deg)	49.4	52.1	52.2	52.1
no. of reflns measd	total: 14574 unique: 9150	total: 9896 unique: 6259	total: 17517 unique: 6792	total: 12824 unique: 4834
<i>R</i> _{int}	0.071	0.022	0.076	0.037
transmn factors	<i>T</i> _{max} = 0.35 <i>T</i> _{min} = 0.26	<i>T</i> _{max} = 0.93 <i>T</i> _{min} = 0.67	<i>T</i> _{max} = 0.907 <i>T</i> _{min} = 0.652	<i>T</i> _{max} = 0.869 <i>T</i> _{min} = 0.684
structure solution			direct methods (SIR92)	
no. of obsd data [<i>I</i> > 3 σ (<i>I</i>)]	7310	5097	3787	3392
no. of params refined	573	337	388	262
reflns/param ratio	12.76	15.12	9.76	12.95
final residuals: <i>R</i> ; <i>R</i> _w ; <i>R</i> _{all} ^a	0.045; 0.046; 0.066	0.029; 0.032; 0.038	0.044; 0.049; 0.092	0.028; 0.036; 0.047
goodness of fit indicator ^b	1.53	1.13	1.32	1.28
max. shift/error final cycle	0.01	0.21	0.01	0.04
max. and min. peaks,	0.73, -1.31	1.21, -1.49	1.20, -1.21	0.91, -0.97
final diff map (e ⁻ /Å ³)				

^a $R = \sum ||F_o| - |F_c|| / \sum |F_o|$; $R_w = [\sum w(|F_o| - |F_c|)^2 / \sum w F_o^2]^{1/2}$. ^b Goodness of fit = $[\sum w(|F_o| - |F_c|)^2 / (N_{\text{obs}} - N_{\text{parameters}})]^{1/2}$.

708 (10, [M - SiMe₃]⁺), 562 (79), 489 (100). Anal. Calcd for C₃₃H₆₂NOSi₄Ta (782.15): C, 50.68; H, 7.99; N, 1.79. Found: C, 50.66; H, 8.31; N, 1.75.

Cp*(DippN=)Ta[¹⁷O=O]Si(SiMe₃)₃Me (24-¹³C). Selected data: ¹³C NMR (126 MHz, benzene-*d*₆): δ 408.6 (q, COSY, *J* = 4). ²⁹Si NMR (99 MHz, benzene-*d*₆): δ -10.0 (d, Si(SiMe₃)₃, *J* = 2), -69.0 (s, Si(SiMe₃)₃). IR (KBr, cm⁻¹): 1391- (w, $\nu^{13}\text{CO}$, from difference spectrum).

[Cp*(DippN=)TaMe(μ -H)]₂ (25). A benzene-*d*₆ (0.5 mL) solution of compound **23** (15 mg, 0.02 mmol) was transferred to an NMR tube fitted with a J. Young Teflon stopper. The NMR tube was then sealed under H₂ (1 atm) and shaken. Within 10 s, the color of the solution had changed from red-orange to light yellow, and a pale yellow precipitate had settled. After 30 min, the solvent and volatile byproducts were removed in vacuo, and the resulting residue was washed with cold (-30 °C) pentane to afford pure **25** (9.5 mg, 94%). ¹H NMR (500 MHz, benzene-*d*₆): δ 7.08, 6.98 (2 × dd, 2 × 2 H, *m*-Ar-H, *J* = 8, 2), 6.90 (br s, 2 H, Ta-H), 6.84 (t, 2 H, *p*-Ar-H, *J* = 8), 4.18, 3.47 (2 × septet, 2 × 2 H, ¹Pr-H, *J* = 7), 1.77 (s, 30 H, C₅Me₅), 1.42, 1.36, 1.31, 0.81 (4 × d, 4 × 6 H, ¹Pr-Me, *J* = 7), 0.43 (s, 6 H, Ta-Me). ¹³C{¹H} NMR (126 MHz, benzene-*d*₆): δ 151.6, 145.0, 144.7 (Ar C), 123.6, 122.9, 122.6 (Ar CH), 114.5 (C₅Me₅), 34.1 (Ta-Me), 27.7, 27.4, 26.9, 26.1, 24.1, 23.6 (¹Pr), 11.4 (C₅Me₅). IR (KBr, cm⁻¹): 1595 (s, br, ν_{TaH}). Anal. Calcd for C₄₆H₇₂N₂Ta₂ (1014.99): C, 54.44; H, 7.15; N, 2.76. Found: C, 54.13; H, 6.84; N, 2.84.

Cp*(DippN=)Ta(CH₂CMe₃)H (26). A freshly prepared solution of Me₃CCH₂MgCl in diethyl ether (1.0 mL, 1.0 M, 1.0

mmol) was added via syringe to a stirred diethyl ether (30 mL) solution of complex **4** (500 mg, 0.47 mmol). After stirring the reaction mixture for 12 h at room temperature, the solvent was removed in vacuo to give a yellow solid, which was extracted with hexanes (30 mL). The extracts were filtered, concentrated to ca. 10 mL, and cooled to -25 °C to afford two crops of yellow cubes of **26** (350 mg, 66%). ¹H NMR (300 MHz, benzene-*d*₆): δ 15.09 (d, 1 H, Ta-H, *J* = 3), 7.21 (t, 2 H, *m*-Ar-H, *J* = 8), 6.96 (t, 1 H, *p*-Ar-H, *J* = 8), 4.15 (br septet, 2 H, ¹Pr-H), 3.04 (d, 1 H, Ta-CH₂, *J* = 12; *J*_{CH} = 115), 1.89 (s, 15 H, C₅Me₅), 1.41, 1.37 (2 × d, 2 × 6 H, ¹Pr-Me, *J* = 7), 1.22 (s, 9 H, CMe₃), -2.21 (dd, 1 H, Ta-CH₂, *J* = 12, 3; *J*_{CH} = 89). ¹³C{¹H} NMR (100 MHz, benzene-*d*₆): δ 151.3, 144.5 (Ar C), 127.0 (Ta-CH₂), 123.3, 122.7 (Ar CH), 116.6 (C₅Me₅), 38.5 (CMe₃), 35.1 (CMe₃), 27.9, 25.2, 25.1 (br, ¹Pr), 11.7 (C₅Me₅). IR (KBr, cm⁻¹): 1753 (m, ν_{TaH}). Anal. Calcd for C₂₇H₄₄NTa (563.60): C, 57.45; H, 7.87. Found: C, 57.45; H, 8.15.

Cp*(DippN=)Ta(CH₂CMe₃)D (26-d). Selected data: IR (KBr, cm⁻¹): 1254 (w, ν_{TaD}).

X-ray Structure Determinations. Single-crystal analysis of all compounds was carried out by Dr. Fred Hollander and Dr. Dana L. Caulder at the College of Chemistry CHEXRAY crystallographic facility at the University of California, Berkeley. Measurements were made on a Bruker SMART CCD area detector with graphite-monochromated Mo K α radiation (λ = 0.71069 Å). Data were integrated by the program SAINT, were corrected for Lorentz and polarization effects, and were analyzed for agreement and possible absorption using XPREP. Empirical absorption corrections were made using SADABS.

Structures were solved by direct methods and were expanded using Fourier techniques. All calculations were performed using the *teXsan* crystallographic software package.

For Compound 5·(THF)₂. Suitable crystals were grown by slow vapor diffusion of pentane into a THF solution of **5** at $-30\text{ }^{\circ}\text{C}$. A yellow polyhedral crystal ($0.20 \times 0.20 \times 0.15\text{ mm}$) was mounted on a quartz fiber using Paratone N hydrocarbon oil and was cooled under a nitrogen stream in the diffractometer. Selected crystal and structure refinement data are summarized in Table 5. The correct enantiomorph (non-centrosymmetric space group) was chosen by Friedel pair analysis. Non-hydrogen atoms were refined anisotropically, except for Li, which was refined isotropically. The hydride (H(60)) was located in the difference Fourier map and was refined isotropically. All other hydrogen atoms were included in calculated idealized positions but were not refined. Hydrogen atoms were not included for the five THF molecules because of the high thermal motion of their carbon atoms. The final refinement cycle converged at $R = 0.045$ and $R_w = 0.046$.

For Compound 6. Suitable crystals were grown from hexane solutions at $-30\text{ }^{\circ}\text{C}$. A red blade-like crystal ($0.30 \times 0.10 \times 0.04\text{ mm}$) was mounted on a quartz fiber using Paratone N hydrocarbon oil and was cooled under a nitrogen stream in the diffractometer. Selected crystal and structure refinement data are summarized in Table 5. Non-hydrogen atoms were refined anisotropically. The hydride (H(1)) was located in the difference Fourier map and was refined isotropically. All other hydrogen atoms were included in calculated idealized positions but were not refined. The final refinement cycle converged at $R = 0.029$ and $R_w = 0.032$.

For Compound 20. Suitable crystals were grown from hexane solutions at $-30\text{ }^{\circ}\text{C}$. A clear tabular crystal ($0.15 \times 0.08 \times 0.20\text{ mm}$) was mounted on a quartz fiber using Paratone N hydrocarbon oil and was cooled under a nitrogen stream in the diffractometer. Selected crystal and structure refinement

data are summarized in Table 5. Non-hydrogen atoms were refined anisotropically. Hydrogen atoms were included but were not refined. All of the hydrogen atoms were placed in calculated positions except for the hydride (H(1)), which was located in the difference Fourier map and was included in its found position. The final refinement cycle converged at $R = 0.044$ and $R_w = 0.049$.

For Compound 26. Suitable crystals were grown from pentane solutions at $-30\text{ }^{\circ}\text{C}$. A fragment ($0.30 \times 0.35 \times 0.25\text{ mm}$) was cut from a yellow blocky crystal, mounted on a quartz fiber using Paratone N hydrocarbon oil, and cooled under a nitrogen stream in the diffractometer. Selected crystal and structure refinement data are summarized in Table 5. Non-hydrogen atoms were refined anisotropically. The hydride (H(1)) was located in the difference Fourier map and was included in that position. All other hydrogen atoms were included in calculated idealized positions but were not refined. The final refinement cycle converged at $R = 0.028$ and $R_w = 0.036$.

Acknowledgment is made to the National Science Foundation for their generous support of this work. U.B. thanks the Schweiz. Nationalfonds and the Novartis Stiftung for postdoctoral fellowships. We thank Dr. Frederick J. Hollander and Dr. Dana L. Caulder for determination of the crystal structures.

Supporting Information Available: Complete IR data; tables of crystal, data collection, and refinement parameters, atomic coordinates, bond distances, bond angles, and anisotropic displacement parameters for compounds **5·(THF)₂**, **6**, **20**, and **26**. This material is available free of charge via the Internet at <http://pubs.acs.org>.

OM0203227